How sharp is the chiral crossover phenomenon for realistic meson masses?

Hildegard Meyer-Ortmanns* and Bernd-Jochen Schaefer†
Institut für Theoretische Physik der Universität Heidelberg, Philosophenweg 19, D-69120 Heidelberg, Federal Republic of Germany
(Received 31 August 1995)

The mass dependence of the chiral phase transition is studied in the linear SU(3)×SU(3) σ model to leading order in a $1/N_f$-expansion, N_f denoting the number of flavors. For realistic meson masses we find a smooth crossover between $T\sim 181.5$ and 192.6 MeV. The crossover looks more rapid in the light quark condensate than in thermodynamic quantities such as the energy and entropy densities. The change in the light quark condensate in this temperature interval is $\sim$ 50% of the zero-temperature condensate value, while the entropy density increases by $(5.5\pm 0.8)\times 10^{-3}$ GeV^3. Since the numerical error is particularly large in this region, we cannot rule out a finite latent heat smaller than 0.2 GeV/fm^3. The chiral transition is washed out for an average pseudoscalar meson octet mass $\geqslant$ 203 MeV. This gives an upper bound on the first-order transition region in the meson mass parameter space. The corresponding ratio of critical to realistic light current quark masses $m_{u,d}^{\rm crit}/m_{u,d}$ is estimated as 0.26 ± 0.08. This result is by an order of magnitude larger than the corresponding mean-field value. Therefore, the realistic quark or meson masses seem to lie less deeply in the crossover region than it is suggested by a mean-field calculation. [S0556-2821(96)05311-8]

PACS number(s): 13.75.Lb, 05.70.Ce, 11.30.Rd, 64.60.Fr

I. INTRODUCTION

Spontaneous symmetry breaking is frequently used as an ansatz to explain the driving force of finite temperature phase transitions in QCD. The symmetries refer to certain limiting cases of the QCD Lagrangian. In the limit of infinite quark masses and in the case of three colors finite temperature QCD is invariant under $Z(3)$ transformations [$Z(3)$ is the center of SU(3)]. The spontaneous breaking of $Z(3)$ is made responsible for the phase transition from the confinement phase at low temperatures to the deconfinement phase at high temperatures. In the other extreme case of N_f vanishing current quark masses QCD is invariant under SU(N_f)× SU(N_f) chiral transformations. The restoration of the spontaneously broken chiral symmetry at high temperatures is said to drive the chiral phase transition of QCD. For the chiral limit the renormalization group analysis of Pisarski and Wilczek [1] serves as a guide for conjectures about the order of the chiral phase transition. Similar studies have been performed by Svetitsky and Yaffe [2] in the other extreme case of pure gauge theory or infinite quark masses.

From numerous numerical simulations in lattice QCD it is known that the order of the QCD transitions is rather sensitive to the approximation scheme. It depends on the number of colors (N_c), the number of flavors (N_f), the bare coupling g (in the staggered fermion formulation of lattice QCD), the size of the volume, and, last but not the least, on the current quark masses in the Lagrangian. Ultimately, one is interested in the physical case of three colors, two light and one heavier flavor ($m_{u,d}\approx 10$ MeV, $m_s\approx 150-200$ MeV) in the space-time continuum for large or infinite volumes. Conjectures about the order of the QCD transitions, in these limiting cases, are no longer conclusive, if the deviations from the symmetric limits of zero or infinite quark masses are large.

In reality, the current quark masses are neither infinite nor zero. The masses of the charm, bottom, and top quarks are large compared to the scale of the critical temperature T_c of QCD, which lies between 150 and 250 MeV. Thus, it seems to be justified to treat them as infinite in thermodynamic investigations. The (renormalization group-invariant current) masses of the up and down quarks are small compared to T_c, $m_u=7.6\pm 2.2$ MeV, $m_d=13.3\pm 3.9$ MeV for $\Lambda=100$ MeV, where Λ refers to the modified minimal subtraction ($\overline{\rm MS}$) scheme with three flavors [3]. At a first glance it seems to be well justified to set them simply to zero, although more careful investigations in the framework of chiral perturbation theory give us a warning not to neglect their influence on the chiral transition [4]. A particular role is played by the strange quark. Its mass ($m_s\sim 205\pm 50$ MeV) is neither small nor large, but just of the order of the scale which is set by T_c.

To get an idea about the influence of finite quark masses on the phase structure of QCD it is instructive to consult statistical physics. The phase transition from a liquid to a gas is of first order below some critical value of the pressure. For a critical value of the pressure it becomes of second order. Above the critical strength it turns into a smooth crossover between the liquid and the gas phase. A crossover phenomenon means a conversion from one phase to the other without any singularity in thermodynamic quantities. Similar effects are known from ferromagnets under the influence of an external magnetic field. In an O(N) ferromagnet an arbitrarily small magnetic field is sufficient to turn the second-order transition with an infinite correlation length into a crossover without a diverging correlation length. In close analogy to our subsequent considerations, we should also mention the three-dimensional $Z(3)$-Potts model. The spin variables of this model can take three values at each lattice site. For a vanishing external magnetic field, the Potts model is known to have a first-order phase transition at finite temperature. For a critical field strength it becomes of second order and disappears for even stronger external fields.

The conjugate variables are the pressure and the specific

*Electronic address: ort@dhdmpi5.bitnet
†Electronic address: schaefer@hybrid.tphys.uni-heidelberg.de

volume in the liquid or gas system, the external magnetic field, and the magnetization for the ferromagnet. The analogous pair in QCD is the current quark masses and the quark condensates as the associated order parameters for the chiral transition on the quark level. On the mesonic level we have external fields rather than quark masses and mesonic condensates rather than quark condensates. The comparison between the statistical systems and QCD goes beyond a formal analogy. In an SU(3) lattice gauge theory it has been shown by DeGrand and DeTar [5] and Banks and Ukawa [6] that dynamical fermions on the QCD level induce an external field coupled linearly to a spin field in an effective $Z(3)$-spin model. The spin model has been *derived* from QCD in a strong coupling expansion at high temperatures. The external field strength was expressed in terms of the hopping parameter of the original lattice-QCD Lagrangian.

Results and conjectures on the mass dependence of the finite temperature transitions have been summarized in the famous Columbia plot [7]. The results refer to Monte Carlo simulations. The plot shows the order of the QCD transitions as a function of the strange and light quark masses in lattice units, $m_s a, m_{u,d} a$, respectively. In particular, the mass point with two light ($m_{u,d} a = 0.025$) and one heavier flavor ($m_s a = 0.1$) is indicated in the crossover region. It refers to a result of [7] which has been obtained within the staggered fermion formulation. This mass point comes closest to the realistic quark masses with a ratio of $m_s / m_{u,d} \approx 20$. The lattice result suggests that the mass point with realistic quark masses is not too far from the second-order transition line, although the precise values of the critical strange quark masses, where the first-order transitions turn into second-order transitions, are still an open question.

Thus, the conclusion from the lattice is that there is no true chiral phase transition for physical quark masses. Depending on the reliability of this result it may have far-reaching consequences in view of measurable effects in heavy-ion collisions. Before jumping to conclusions in this direction one should keep in mind the limitations of lattice calculations.

Lattice results are in general affected by artefacts because of the finite IR cutoff in numerical simulations, the UV cutoff (i.e., the finite lattice constant) and finite bare quark masses. Since the mass point with two light and one heavier flavor has been obtained for a lattice extension of only four slices in the imaginary time direction, the result may not yet reflect continuum physics. A further obstacle in the staggered fermion formulation applies, in particular, to the case of three flavors. The effective fermionic action, which projects on three flavors, must be regarded as a prescription; it cannot be derived from the staggered fermion action. The error because of this prescription seems to be difficult to control. These warnings should suffice as arguments in favor of alternative approaches, which include different approximations, to study the phase structure of QCD. Such alternative approaches are *effective models*.

In this paper, we consider the $SU(3) \times SU(3)$ linear σ model as an effective model for QCD in the low temperature phase for temperatures T up to the scale of T_c. The linear σ model has been extensively discussed in the renormalization group analysis of Pisarski and Wilczek [1] as the most general renormalizable effective model sharing the chiral symmetry properties with QCD. We assume that the restoration of the spontaneously broken $SU(3) \times SU(3)$ symmetry is the driving mechanism for the chiral phase transition. The deviations in the spectrum from the idealized octet of pseudoscalar Goldstone bosons are parametrized by terms which break the $SU(3) \times SU(3)$ symmetry explicitly. We include two external fields to account for the finite quark masses on the mesonic level. The assumption in our decimation of degrees of freedom is that only mesons associated with the $SU(3) \times SU(3)$ multiplets are important for the phase transition. The criterion is chiral symmetry rather than the size of the meson masses.

The action is constructed in terms of QCD's chiral order parameter field M, where M is a complex 3×3 matrix. It may be regarded in analogy to Landau's free energy functional F. Landau's free energy functional is also constructed in terms of an order parameter field to describe the phase structure of a system in statistical physics. In the special case of one external field and one mesonic condensate, the action of the σ model takes the form of Landau's free energy functional for a liquid-gas system (cf. Sec. V). Thus, we expect the same qualitative features as we know from the liquid-gas system. Beyond certain critical values of the meson masses, the chiral transition should be washed out and turned into a crossover phenomenon with smooth changes in the condensates, energy density, and entropy density. Therefore, the main question is, as to whether the realistic quark masses are too large for the chiral transition to persist.

In [8] a systematic study of the mass dependence of the chiral transition has been proposed in the framework of the $SU(3) \times SU(3)$ linear σ model. In a first paper [8], a loose bound on the first-order transition region was given in terms of the (average) pseudoscalar octet mass. It was 100 MeV for a σ meson mass between 600 and 950 MeV. The qualitative conclusion was that realistic meson masses lie deeply in the crossover region. The results were obtained in a large N_f expansion under the omission of $n \neq 0$ Matsubara frequencies. Here, we still use the large N_f expansion, but include all Matsubara frequencies, as the omission of the $n \neq 0$ modes seems to be justified only for high temperatures and in the case of a second-order phase transition.

Our main topic is to find a quantitative answer to the following two questions. The first one refers to the particular tri- or multicritical mass values for which the chiral transition is of second order even in the case of three flavors [with $SU(3) \times SU(3)$ symmetry in the chiral limit]. Once these values are known, it is of interest how far the physical quark or meson masses are from critical masses. This distance (in mass parameter space) is more than a quantity of academic interest. Its physical relevance can be seen as follows. Assume that the physical masses are not identical but very close to the critical mass values where the chiral transition is of second order. The ratio of critical to physical light current quark masses $m_{u,d}^{\mathrm{crit}} / m_{u,d}$ would be close to 1.

There are several reasons why a ratio $m_{u,d}^{\mathrm{crit}} / m_{u,d} \approx 1$ is quite attractive. First of all, the chances are then good to see some remnant in heavy-ion collisions of a diverging correlation length for critical mass values, i.e., a rather large correlation length for realistic masses. One manifestation of a large correlation length has been supposed to be large clusters of charged or neutral pions which are aligned in isospin

space [9]. The correlation volume of a cluster should be large enough so that the number of emitted pions is sufficient for the detector to resolve the cluster structure.

Also from a theoretical point of view an almost second-order chiral transition in the presence of finite quark masses is very appealing, because it justifies the decimation of QCD to a σ model, when both theories share the same universality class. Finally, a finite mass scaling analysis for a second-order transition could be performed with physical masses as ''perturbations'' of (tri-)critical masses. A finite mass scaling analysis has been used by Boyd *et al.* [10] for the case of *two massless* flavors in the chiral limit, see also [11]. As long as the strange quark mass is implicitly set to infinity for two massless flavors, we do not expect a final answer from such type of investigation. This is the reason why we have favored $SU(3)\times SU(3)$.

The second question has been raised in the title: How sharp is the chiral crossover phenomenon for realistic meson masses? Also, the vicinity of the first-order transition region could leave observable effects if the crossover for realistic masses is still sharp enough. A sharp crossover is associated with a rapid change in the condensates and their induced masses, and/or a rapid change in the entropy and energy densities in a small temperature interval. In our case this interval turns out to be $\approx 182-192$ MeV, (cf. Sec. VI). It makes then still some sense to call the ''midpoint'' of this interval of rapid change ''T_c.'' Average transverse momentum distributions of charged particles could be flattened as a function of the multiplicity dN/dy of final state particles in a given rapidity interval [12]. Pronounced fluctuations in the particle multiplicities would show up, if the crossover is strong enough to induce deflagration processes during the phase conversion [13]. True singularities of a first- or second-order transition will be anyway rounded in real experiments because of the finite volume.

On the other hand, a ratio $m_{u,d}^{\rm crit}/m_{u,d}$ of 3% (cf. our mean-field result in Sec. V) would mean that there should not be any remnant of the singularity structure of the transition in the chiral limit. Experimentalists should not be surprised not to see any ''effect'' of a hypothetical phase transition.

If the physical masses turn out to lie far outside the first-order transition region, nonuniversal features of the σ model may influence the results, and predictions from this model are of little impact on real experiments.

It may be academic to ask as to whether chiral symmetry restoration in the infinite volume limit proceeds via a weakly first-order transition or a smooth crossover phenomenon. In view of physical applications, it is certainly more sensible to pose the question in the following way: Is the gap in entropy densities in the transition or crossover region sufficient to induce multiplicity fluctuations in the observed pion yield, lying clearly above the statistical noise? A reliable answer to this question can be expected only from full QCD. In this paper, we try to give a partial answer: Which part of the total (yet unknown) gap in the entropy and energy densities comes from chiral symmetry? We find a quantitative measure for how sharp the chiral crossover phenomenon is for realistic meson masses if gluonic degrees of freedom are completely neglected.

The paper is organized as follows. In Sec. II we introduce the tree-level parametrization of the $SU(3)\times SU(3)$ linear σ model at zero temperature. We give a prescription to translate the meson condensates and meson masses to quark condensates and quark masses. In Sec. III we summarize the essence of our approach. The mesonic self-interaction is treated to leading order in an expansion in the number of quark flavors N_f. On the mesonic level we have nine scalar plus nine pseudoscalar mesons. The $SU(3)\times SU(3)$ σ model reduces to an O(18) model in the limit of two vanishing couplings. Thus, the leading order of a $1/N$ expansion should be a good starting point. The thermodynamic effective potential is evaluated in a high-temperature expansion and in a fully numerical approach. The numerical approach is certainly more appropriate to the phase transition region. To discuss the mass dependence of the order of the chiral transition we distinguish three regions in mass parameter space: the chiral limit (Sec. IV), several mass points on the first-order transition boundary, so-called critical mass points (Sec. V), and realistic meson masses (Sec. VI), which come close to the experimental masses. We describe the crossover phenomenon in the meson and quark condensates as a function of temperature. The crossover is also manifest in thermodynamic quantities such as the energy density ε, the entropy density s, and the pressure p. We derive ε, s and p from the partition function of the σ model in a saddle-point approximation. Upper bounds on a finite latent heat during the chiral transition are predicted. In Sec. VII we summarize our results and draw some conclusions in view of physical applications.

II. TREE-LEVEL PARAMETRIZATION OF THE SU(3)×SU(3) LINEAR σ MODEL

The Euclidean Lagrangian density of the $SU(3)\times SU(3)$ linear σ model is given as

$$\mathcal{L}=\frac{1}{2}\mathrm{Tr}(\partial_\mu M\partial_\mu M^+)-\frac{1}{2}\mu_0^2\mathrm{Tr}MM^+ +g(\det M+\det M^+)$$
$$+f_1(\mathrm{Tr}MM^+)^2+f_2\,\mathrm{Tr}(MM^+)^2-\varepsilon_0\sigma_0-\varepsilon_8\sigma_8, \quad (1)$$

where the (3×3)-matrix field $M(x)$ is written as

$$M=\frac{1}{\sqrt{2}}\sum_{\ell=0}^{8}(\sigma_\ell+i\pi_\ell)\lambda_\ell. \quad (2)$$

Here, σ_ℓ and π_ℓ denote the nonets of scalar and pseudoscalar mesons, respectively, λ_ℓ ($\ell=1,\ldots,8$) are the Gell-Mann matrices, $\lambda_0=\sqrt{2/3}[\mathrm{diag}(1,1,1)]$. The chiral $SU(3)\times SU(3)$ symmetry is explicitly broken by the term $(-\varepsilon_0\sigma_0-\varepsilon_8\sigma_8)$, which is linear in the external fields $\varepsilon_0,\varepsilon_8$. A nonvanishing value of ε_0 gives a common mass value to the octet of pseudoscalar Goldstone bosons m_π, m_k, m_η. When also $\varepsilon_8\neq 0$, it can be adjusted such that it leads to a realistic mass splitting inside the (pseudo)scalar meson octets.

The Lagrangian (1) appears as a natural candidate for an effective model, which is designed to describe the phenomenon of chiral symmetry restoration. If the mass parameters are chosen to induce a second-order phase transition, the action $S=\int d^3x d\tau\mathcal{L}(x)$ with $\mathcal{L}$ of Eq. (1) may be regarded as a candidate for an effective action for QCD. It is constructed

in terms of a chiral order parameter field M for the chiral transition and is supposed to share its universality class with QCD. As order parameters for the chiral transition, we choose the meson condensates $\langle\sigma_0\rangle$ and $\langle\sigma_8\rangle$. The expectation value of M is then parametrized in terms of $\langle\sigma_0\rangle,\langle\sigma_8\rangle$ according to

$$\langle M\rangle = \mathrm{diag}\frac{1}{\sqrt{3}}\left[\langle\sigma_0\rangle+\frac{1}{\sqrt{2}}\langle\sigma_8\rangle,\langle\sigma_0\rangle+\frac{1}{\sqrt{2}}\langle\sigma_8\rangle,\langle\sigma_0\rangle-\sqrt{2}\langle\sigma_8\rangle\right]. \tag{3}$$

The construction of an action S in terms of an order parameter field is a concept in close analogy to Landau's free energy functional $\mathcal{F}$ in terms of an order parameter field, $\mathcal{F}$ coincides with S in the mean-field approximation. Quartic terms in M have to be introduced in Eq. (1) to allow for the possibility of spontaneous symmetry breaking. For $g=0=\varepsilon_0=\varepsilon_8$ the Lagrangian is still invariant under U(3) $\times$U(3) transformations. For $N_f\geqslant 3$ there are two independent quartic terms, parametrized with coefficients f_1 and f_2. To account for a realistic (η,η')-mass splitting, a det-term with an ''instanton''-coupling g has to be included as well. It reduces the symmetry of $\mathcal{L}$ to SU(3)$\times$SU(3) if $\varepsilon_0=0=\varepsilon_8$. Finally, the external field terms which are linear in M are the most simple choice for an explicit symmetry breaking accounting for the small, but finite masses of the Goldstone octet (m_π,m_K,m_η). Thus, one arrives at the SU(3)$\times$SU(3) linear σ model in a natural way if one is interested in the limited aspect of chiral symmetry restoration approaching the transition region from below.

It remains to fix the Lagrangian parameters $\mu_0^2,f_1,f_2,g,\varepsilon_0,\varepsilon_8$ from an experimental input. The choice of the input and the way of parametrization are in no way unique, cf. [14,15,8]. Since the pseudoscalar meson masses are experimentally well known, $m_\pi,m_k,m_\eta,m_{\eta'}$, and f_π have been used in [8] to fix $\mu_0^2,f_1,f_2,g,\varepsilon_0$, and ε_8. In addition, the mass of the σ' meson has been treated as input parameter and varied between 600 and 950 MeV to solve for μ_0^2 and f_1, which occur in the (pseudo)scalar meson masses in the combination $[-\mu_0^2+4f_1(\sigma_0^2+\sigma_8^2)]$. It is worth noting that the order parameters $\langle\sigma_0\rangle,\langle\sigma_8\rangle$ can be determined without knowing μ_0^2 and f_1 separately. The equations for $\mu_0^2,f_1,f_2,g,\varepsilon_0,\varepsilon_8$ do not admit solutions for an arbitrary choice of $m_\pi,m_k,m_\eta,m_{\eta'},f_\pi$, and $m_{\sigma_{\eta'}}$. This was the reason why the input masses which have been actually used as input in [8] were slightly deviating from the experimental values if $m_{\sigma_{\eta'}}$ was chosen as 600 or 950 MeV. In [16] the experimental values could be used for $m_\pi,m_k,m_\eta,m_{\eta'},f_\pi$ on the price that $m_{\sigma_{\eta'}}$ was used as input with 1400 MeV.

In this paper, our interest goes beyond the point with (almost) experimental pseudoscalar meson masses. As we focus on the aspect of the mass sensitivity, we have to find a prescription how to tune the masses in the high-dimensional meson mass parameter space. On the quark level the mass parameter space is only two dimensional, the two parameters being $m_{u,d}$ and m_s. Not only the parametrization, but also the tuning in the space of meson masses is by far not unique. The idea now is to parametrize the (pseudo)scalar meson masses by two parameters such as the quark masses, hereby the external fields ε_0 and ε_8.

A relation between $m_{u,d},m_s$ and $\varepsilon_0,\varepsilon_8$ is obtained by identifying terms of the Lagrangian on the mesonic and on the quark level which transform identically under SU(3) $\times$SU(3). We have

$$(-\varepsilon_0\sigma_0-\varepsilon_8\sigma_8) \quad \text{on the mesonic level,} \tag{4}$$

$$(m_u\overline{uu}+m_d\overline{dd}+m_s\overline{ss}) \quad \text{on the quark level.} \tag{5}$$

Thus, we find

$$-\varepsilon_0=\alpha(2\hat{m}+m_s),$$
$$-\varepsilon_8=\beta(\hat{m}-m_s). \tag{6}$$

Here, α and β are constants. They can be fixed from the known values of $\varepsilon_0,\varepsilon_8,m_{u,d}$, and m_s under realistic conditions. Realistic meson masses are obtained for $\varepsilon_0=0.0265\ \mathrm{GeV}^3,\varepsilon_8=-0.0345\ \mathrm{GeV}^3$, see below. The values for ''realistic'' current quark masses are taken from [17], $\hat{m}\equiv(m_u+m_d)/2=11.25\pm1.45$ MeV, $m_s=205\pm50$ MeV. For α and β we then obtain

$$\alpha=-0.1164\ \mathrm{GeV}^2,\quad \beta=-0.1780\ \mathrm{GeV}^2. \tag{7}$$

Thus, a variation in $(\varepsilon_0,\varepsilon_8)$ can be mapped onto a variation of $(\hat{m},m_s)$.

Next, we have to find a mapping between $(\varepsilon_0,\varepsilon_8)$ and the (pseudo)scalar meson masses. As it is possible to explain the variety of (pseudo)scalar meson masses on the basis of two quark masses $m_{u,d}$ and m_s, it should be similarly possible to reach any point in an $(m_\pi,m_{K,\ldots})$ diagram by a variation of ε_0 and ε_8. Thus, we start with the parametrization of the chiral limit $\mu_0^2,f_1,f_2,g,\varepsilon_0=0$, $\varepsilon_8=0$, keep the couplings μ_0^2,f_1,f_2,g fixed and switch on $\varepsilon_0\neq0$, $\varepsilon_8\neq0$. The SU(3) symmetric case with finite, but degenerate pseudoscalar meson masses is obtained for $\varepsilon_0\neq0$, $\varepsilon_8=0$. The mass point with realistic meson masses which come close to their experimental values, is obtained for $\epsilon_0=0.0265\ \mathrm{GeV}^3$, $\varepsilon_8=-0.0345\ \mathrm{GeV}^3$ as mentioned above. (In principle, there is no obstacle to further optimize the values of $\varepsilon_0,\varepsilon_8$ such that they do reproduce the experimental mass values.) For the chiral values μ_0^2,f_1,f_2,g and a certain choice for ε_0 and ε_8, we first determine $\langle\sigma_0\rangle$ and $\langle\sigma_8\rangle$, the condensates at zero temperature, as zeros of (8) and (9) in σ_0 and σ_8:

$$\varepsilon_0+\mu_0^2\sigma_0-\frac{g}{\sqrt{3}}(2\sigma_0^2-\sigma_8^2)+\frac{2\sqrt{2}}{3}f_2\sigma_8^3-4\left(f_1+\frac{f_2}{3}\right)\sigma_0^3-4(f_1+f_2)\sigma_0\sigma_8^2=0, \tag{8}$$

$$\varepsilon_8+\mu_0^2\sigma_8+\sqrt{\frac{2}{3}}g(\sigma_8^2+\sqrt{2}\sigma_0\sigma_8)+2\sqrt{2}f_2\sigma_0\sigma_8^2-4\left(f_1+\frac{f_2}{2}\right)\sigma_8^3-4(f_1+f_2)\sigma_0^2\sigma_8=0. \tag{9}$$

Equations (8) and (9) are the equations of motion for constant background fields σ_0, σ_8. The pseudoscalar meson masses are then given in terms of μ_0^2, f_1, f_2, g and as functions of the condensates $\langle\sigma_0\rangle, \langle\sigma_0\rangle$. The resulting masses together with the input parameters are listed in Table II of Sec. VI.

To facilitate a comparison with other work on the chiral phase transition, it remains to translate the results for the meson condensates to the quark level. If we identify terms in the Lagrangians on the quark level and on the mesonic level [cf. Eqs. (4) and (5)], we find

$$\frac{1}{3}(2\hat{m}+m_s)(2\overline{qq}+\overline{ss})=-\varepsilon_0\sigma_0, \tag{10}$$

$$\frac{2}{3}(\hat{m}-m_s)(\overline{qq}-\overline{ss})=-\varepsilon_8\sigma_8, \tag{11}$$

with $\overline{qq}=\frac{1}{2}(\overline{uu}+\overline{dd})$, leading to

$$\langle\overline{qq}\rangle=\frac{-\varepsilon_0}{2\hat{m}+m_s}\langle\sigma_0\rangle+\frac{-\varepsilon_8}{2(\hat{m}-m_s)}\langle\sigma_8\rangle,$$

$$\langle\overline{ss}\rangle=\frac{-\varepsilon_0}{2\hat{m}+m_s}\langle\sigma_0\rangle+\frac{+\varepsilon_8}{\hat{m}-m_s}\langle\sigma_8\rangle. \tag{12}$$

The coefficients are just proportional to α and $\pm\beta$, as a comparison with Eq. (6) shows; α and β have been determined in Eq. (7). Later, we take the relations (12) as temperature independent and substitute $\langle\sigma_0\rangle(T), \langle\sigma_8\rangle(T)$ for the corresponding condensates at zero temperature. This assumption is consistent with our approach. We also treat the couplings μ_0^2, f_1, f_2, g of the Lagrangian as temperature independent. Therefore, the symmetry of $\mathcal{L}$ remains unchanged under an increase of T. The symmetry was on the basis of the identification which has led to Eqs. (12). (The assumption of temperature-independent couplings may not be justified in the vicinity of the transition region.) In the next section we will outline how to calculate $\langle\sigma_0\rangle(T), \langle\sigma_8\rangle(T)$.

III. LARGE-N_f EXPANSION

In an earlier calculation the linear SU(3)×SU(3) σ model has been considered in a mean-field approximation [18]. Recently, Gavin, Gocksch, and Pisarski [15] have tried to localize the first-order transition boundary in an $(m_{u,d}, m_s)$-mass diagram in a *mean-field* calculation. The famous renormalization group analysis of Pisarski and Wilczek [1] applied to the linear σ model in the *chiral limit*. Frei and Patkós [19] were the first to apply a saddle-point approximation to the partition function of the σ model. Their investigations were also restricted to the chiral limit. Meyer-Ortmanns, Pirner, and Patkós [8] have extended the approach of Frei and Patkós to finite meson masses. In [8] only the zero-Matsubara frequencies were kept. When the imaginary time dependence of the fields or, equivalently, the $n\neq 0$-Matsubara frequencies are dropped, it results in a dimensional reduction of the four-dimensional theory to an effective three-dimensional theory. In general, such a reduction can be justified in the high-T limit or for an anticipated second-order phase transition. In both cases the ratio of β/ξ is negligible (β is the inverse temperature and ξ denotes the largest correlation length of the system). The $n\neq 0$-Matsubara modes were included in [16]. In this paper, we follow the same approach as in [16], but extend the work to study the aspect of the mass sensitivity of the chiral transition. Further differences in details of [16] and the present paper will be mentioned below. In the following, we summarize the main steps of our approach.

The temperature-dependent order parameters are the meson condensates $\langle\sigma_0\rangle(T)$ and $\langle\sigma_8\rangle(T)$. They are related to the light and strange quark condensates according to Eqs. (12). The values of $\langle\sigma_0\rangle(T), \langle\sigma_8\rangle(T)$ are determined as the minima of an effective potential $\hat{U}_{\rm eff}(\sigma_0,\sigma_8)$. The effective potential is calculated as a constrained free energy density, i.e., the free energy density under the constraint that the average fields $1/\beta V\int_0^\beta d\tau\int d^3x\,\sigma_{0,8}(\vec{x},\tau)$ take prescribed values $\overline{\sigma_0}$ and $\overline{\sigma_8}$, respectively, while the same averages over $\sigma_\ell, \ell=1,\ldots,7$ and $\pi_\ell, \ell=0,\ldots,8$ should vanish. The physical meaning is obvious. If one chooses $\overline{\sigma_0}, \overline{\sigma_8}\neq 0$ in the high-temperature chiral symmetric phase, the corresponding free energy is certainly not minimal for such a choice. We consider spontaneous symmetry breaking in two directions. Accordingly, we introduce two background fields $\overline{\sigma_0}, \overline{\sigma_8}$:

$$\sigma_0=\overline{\sigma_0}+\sigma_0',$$

$$\sigma_8=\overline{\sigma_8}+\sigma_8', \tag{13}$$

where σ_0', σ_8' denote the fluctuations around the background. Otherwise, $\sigma_\ell=\sigma_\ell'$ for $\ell=1,\ldots,7$ and $\pi_\ell=\pi_\ell'$ for $\ell=0,\ldots,8$. As a common notation for σ_ℓ', π_ℓ' we use $M_\ell'=\overline{\sigma_\ell'}+i\overline{\pi_\ell'}$. The actual minima of $\hat{U}_{\rm eff}(\sigma_0,\sigma_8)$ (with $\sigma_0=\overline{\sigma_0}, \sigma_8=\overline{\sigma_8}$) are denoted as $\langle\sigma_0\rangle$ and $\langle\sigma_8\rangle$.

The Lagrangian is expanded in powers of M_ℓ'. The linear term in M_ℓ' vanishes because of the δ constraint in the constrained-free energy density. The quadratic term defines the masses m_Q^2 of the meson multiplets $\pi, K, \eta, \eta', \sigma_\pi, \sigma_K, \sigma_\eta, \sigma_{\eta'}$, and $Q=1,\ldots,8$ labels the multiplets. The two quartic terms are quadratized by introducing an auxiliary matrix field $\Sigma(x)$ according to [19]

$$\exp\{-\beta[f_1(\mathrm{Tr}M'M'^{+})^2+f_2\mathrm{Tr}(M'M'^{+})^2]\}$$

$$=\mathrm{const}\times\int_{c-i\infty}^{c+i\infty}\mathcal{D}\Sigma(x)\exp\{\,\mathrm{Tr}\Sigma^2+2\varepsilon\mathrm{Tr}(\Sigma M'M'^{+})$$

$$+2\alpha\mathrm{Tr}(M'M')\mathrm{Tr}\Sigma\}, \tag{14}$$

where $M'(x)$ is an $N\times N$-matrix field and

$$\varepsilon^2=\beta f_2,$$

$$2\varepsilon\alpha+3\alpha^2=\beta f_1.$$

Note that Eq. (14) is a sophisticated version of the simpler case, where ϕ is a scalar field

$$\text{const}\times\exp\{-\alpha[\phi^2(x)]^2\}$$

$$=\int_{c-i\infty}^{c+i\infty}\mathcal{D}\Sigma(x)e^{\Sigma^2(x)-\Sigma(x)\phi^2(x)2\sqrt{\alpha}}. \tag{15}$$

Formula (15) can be easily generalized to the case, where the left-hand side (LHS) includes also a cubic term $\phi^3(x)$, but we are not aware of an analogous transformation that leads to a tractable expression if the cubic term occurs in the form of a determinant. This is the reason why we drop the cubic term in $M'_{\not}$ in the following procedure. The (3×3)-matrix field $\Sigma(x)$ is replaced by an SU(3) symmetric diagonal matrix $\Sigma=\text{diag}(sad,sad,sad)$. Thus the matrix of auxiliary fields is reduced to a single field variable $sad(x)$.

In the saddle-point approximation the path integral $\int\mathcal{D}\Sigma(x)$ is dropped and the auxiliary field $sad(x)$ is replaced by sad^*, which maximizes the integrand. For an O(N) model it is well known that this approximation corresponds to the leading order in a $1/N$ expansion [20]. In the special case of $f_2=0=g$, the SU(3)$\times$SU(3) σ model becomes an O(16) model, which is invariant under O(18) rotations. We have $N=18=2N_f^2$, where N_f denotes the number of quark flavors, while N labels the number of mesonic modes. Terms of O($1/N$) are dropped, as long as fluctuations in the auxiliary field are neglected. Thus we call our scheme a *large-N_f approximation*.

The resulting one-loop contribution to the free energy density is given as

$$-\frac{1}{\beta V}\ln Z=\frac{1}{2\beta}\sum_{Q=1}^{8}g(Q)\sum_{n\in Z}\int\frac{d^3K}{(2\pi)^3}\ln[\beta^2(\omega_n^2+\omega_Q^2)], \tag{16}$$

where $g(\pi)=3,g(K)=4,g(\eta)=1,g(\eta')=1,g(\sigma_\pi)=3,$ $g(\sigma_K)=4,g(\sigma_\eta)=1,g(\sigma_{\eta'})=1$ are the multiplicity factors of the multiplets, $\omega_n^2\equiv(2\pi n/T)^2$ and

$$\omega_Q^2\equiv K^2+X_Q^2$$

$$X_Q^2\equiv sad+\mu_0^2+m_Q^2. \tag{17}$$

Thus the one-loop contribution to the free energy takes a form, which is familiar from a free field theory. The only remnant of the interaction is hidden in the effective mass square X_Q^2 via the auxiliary field variable sad. After the sum over the Matsubara frequencies is performed, the full expression for the effective potential is given as

$$U_{\text{eff}}(\sigma_0,\sigma_8,sad)=U_{\text{class}}(\sigma_0,\sigma_8)+U_{\text{saddle}}(sad)+U_0(\sigma_0,\sigma_8,sad)+U_{\text{th}}(\sigma_0,\sigma_8,sad), \tag{18}$$

where $\sigma_0=\overline{\sigma_0},\sigma_8=\overline{\sigma_8}$ and

$$U_{\text{class}}(\sigma_0,\sigma_8)=-\frac{1}{2}\mu_0^2(\sigma_0^2+\sigma_8^2)+\frac{g}{3\sqrt{3}}(2\sigma_0^3-\sqrt{2}\sigma_8^3-3\sigma_0\sigma_8^2)-\frac{2\sqrt{2}}{3}f_2\sigma_0\sigma_8^3+\left(f_1+\frac{f_2}{3}\right)\sigma_0^4+\left(f_1+\frac{f_2}{2}\right)\sigma_8^4+2(f_1+f_2)\sigma_0^2\sigma_8^2-\varepsilon_0\sigma_0-\varepsilon_8\sigma_8 \tag{19}$$

is the classical part of the potential, which is independent of sad;

$$U_{\text{saddle}}(sad)=-\frac{3}{8(3f_1+f_2)}\left(\frac{sad^2}{2}+\mu_0^2 sad\right) \tag{20}$$

results from the transformation (14). The one-loop part consists of the zero-point energy U_0 and the thermal part U_{th}, given by

$$U_0(\sigma_0,\sigma_8,sad)=\frac{1}{2}\sum_{Q=1}^{8}g(Q)\int^{\Lambda}\frac{d^3K}{(2\pi)^3}\omega_Q, \tag{21}$$

U_0 is divergent if the three-momentum cutoff Λ is sent to infinity, while U_{th} is convergent for $\Lambda\to\infty$ and vanishes for $T=0$:

$$U_{\text{th}}=\frac{1}{\beta}\sum_{Q=1}^{8}g(Q)\int\frac{d^3K}{(2\pi)^3}\ln(1-e^{-\beta\omega_Q}). \tag{22}$$

Our results have been obtained for the potential $\hat{U}_{\text{eff}}\equiv U_{\text{eff}}-U_0$, where the divergent zero-point energy has been dropped. It is often argued that the omission of the zero-point energy is justified if one is finally interested in thermodynamic quantities, which are derived as derivatives of $\ln Z$ with respect to β. Usually, U_0 does not depend on T, and the splitting of the one-loop part of U_{eff} according to U_0 and U_{th} is a splitting in a T-independent and a T-dependent part. Thus, the contribution of U_0 should have no effect on the thermodynamics. We cannot use this argument because U_0 of Eq. (21) has an implicit temperature dependence hidden in X_Q^2 via $sad(T)$, the temperature-dependent saddle-point variable, which is finally chosen such that it maximizes $\hat{U}_{\text{eff}}$ for $sad=sad^*$. This was one of the reasons why the U_0 term was kept in [16]. A renormalization prescription was imposed such that the strong (quartic) cutoff dependence of U_0 was weakened to a $1/\Lambda^2$ dependence. Further differences to [16] are because of corrections of two errors in [16]. After we had removed the programming error in U_{class} of [16], we found two branches in the free energy density f (or the pressure). The branches in f of the high- and low-temperature phases did not cross at some temperature $T=T_c$, although the free energy should behave as a smooth function in T by general thermodynamic arguments. The reason was that the two minima of the potential which exist below $T=200$ MeV were erroneously associated with the true minima in the high- and low-temperature phases. It was not realized that for all temperatures up to $T\leqslant200$ MeV

one minimum is only a local one, while the other one stays the absolute minimum for all temperatures up to $T \geqslant 200$ MeV.

Thermodynamic quantities. Thermodynamic observables are derived from the free energy density $f = \lim_{V\to\infty}(-(1/\beta V)\ln Z)$ in the standard way. The partition function Z is approximated as

$$\hat{Z}(\langle\sigma_0\rangle,\langle\sigma_8\rangle) = e^{-\beta V \hat{U}_{\rm eff}(\langle\sigma_0\rangle(T),\langle\sigma_8\rangle(T);sad^*(T))}. \quad (23)$$

Evaluation of $\hat{U}_{\rm eff}$. Next, let us discuss the evaluation of $\hat{U}_{\rm eff}$ in a little more detail. The expression for $\hat{U}_{\rm eff}$ is familiar from the expression for a free field theory. In a high-temperature expansion it reads

$$\hat{U}_{\rm eff} = U_{\rm class} + U_{\rm saddle} - \frac{T^4}{2\pi^2}\sum_{Q=1}^{8} g(Q)\left\{ \frac{\pi^4}{45} - \frac{\pi^2}{12} y_Q^2 + O(y_Q^3)\right\} \quad (24)$$

with $y_Q = X_Q/T$.

At high temperature the SU(3)×SU(3) linear σ model certainly fails to describe the quark-gluon plasma phase. The critical temperature falls neither in a high- nor in a low-temperature region, the expansion parameter is of order 1 or larger. Nevertheless, we have used the high-temperature expansion, which has been frequently applied in calculations of a thermodynamic potential. It has the advantage that imaginary parts of $\hat{U}_{\rm eff}$ are absent to leading order in X_Q/T, cf., e.g., [21]. We have performed a high-temperature expansion for two sets of mass parameters, the chiral limit and the realistic mass point, see Secs. IV and VII. This way we got some qualitative insight in the phase structure before we could handle the problems in a fully numerical evaluation of $\hat{U}_{\rm eff}$. Analytic expressions for a low-temperature expansion of $\hat{U}_{\rm eff}$ are known as well [22]. We have used them only in intermediate steps to check the numerics.

At a first glance the numerical evaluation of $\hat{U}_{\rm eff}$ looks rather straightforward. For each pair of (σ_0,σ_8) we have to find sad^* that maximizes $\hat{U}_{\rm eff}$. The condensates $\langle\sigma_0\rangle,\langle\sigma_8\rangle$ are then determined as minima of $\hat{U}_{\rm eff}(\sigma_0,\sigma_8;sad^*(\sigma_0,\sigma_8))$. It is well known [21] that the arguments $(K^2+X_Q^2)$ of the logarithm in $\hat{U}_{\rm eff}$ can become negative and lead to imaginary parts in $\hat{U}_{\rm eff}$, which we have mentioned above. The original hope was that the positive contribution of the auxiliary field sad to the masses m_Q helps in avoiding imaginary parts of $\hat{U}_{\rm eff}$.

Actually, no imaginary parts have been found in [19]. The contribution of sad^* to X_Q^2 increases with T, it is positive for $T \geqslant 116$ MeV, but in our case the positive contribution is not sufficient to avoid negative X_Q^2 completely, i.e., for all σ_0,σ_8, and T. It has turned out that the actual minima $\langle\sigma_0\rangle$, $\langle\sigma_8\rangle$ lie always in the ''allowed'' region of real valued $\hat{U}_{\rm eff}$, or at least at the boundary of this region, but on the way of searching the maximum in sad^* and the minima in $\langle\sigma_0\rangle,\langle\sigma_8\rangle$ the routines encounter negative mass squares indispensably. Therefore, $\hat{U}_{\rm eff}$ is analytically continued. The integral in $U_{\rm th}$ of $\hat{U}_{\rm eff}$ is of the type

$$I(z) = \int_0^\infty dx\{x^2 \ln[1-\exp(-(x^2+z^2)^{1/2})]\} = -z^2\sum_{n=1}^{\infty}\frac{1}{n^2}K_2(nz), \quad (25)$$

where K_2 is a modified Bessel function. The analytic continuation of $K_m(nz)$ to complex values of nz is given as

$$K_m(nz) = i^{m+1}\left(\frac{\pi}{2}\right)[J_m(inz) + iY_m(inz)], \quad (26)$$

where J_m are Bessel functions of the first kind and Y_m are Weber functions [23]. This leads to the following form of $\hat{U}_{\rm eff}$:

$$\hat{U}_{\rm eff} = U_{\rm class} + U_{\rm saddle} + \frac{T^4}{2\pi^2}\sum_{Q=1}^{8} g(Q) \times\left\{ \frac{-X_Q^2}{T^2}\sum_{n=1}^{\infty}\frac{1}{n^2}K_2\left(\frac{n}{T}X_Q\right)\right\} \quad (27)$$

for $X_Q^2 \geqslant 0$. For $X_Q^2 < 0$ and $X_Q = \pm i\sqrt{|X_Q^2|}$

$$\hat{U}_{\rm eff} = U_{\rm class} + U_{\rm saddle} + {\rm Re}U_{\rm th} + i\,{\rm Im}U_{\rm th}$$

with

$${\rm Re}U_{\rm th} = \frac{T^4}{2\pi^2}\sum_{Q=1}^{8} g(Q)\left\{ \frac{\pi}{2}\frac{|X_Q^2|}{T^2}\sum_{n=1}^{\infty}\frac{1}{n^2}Y_2\left(\frac{n}{T}|X_Q^2|^{1/2}\right)\right\},$$

$${\rm Im}U_{\rm th} = \frac{T^4}{2\pi^2}\sum_{Q=1}^{\infty} g(Q)\left\{ \pm\frac{\pi}{2}\frac{|X_Q^2|}{T^2}\sum_{n=1}^{\infty}\frac{1}{n^2}J_2\left(\frac{n}{T}|X_Q^2|^{1/2}\right)\right\}. \quad (28)$$

The condensate values $\langle\sigma_0\rangle(T),\langle\sigma_8\rangle(T)$ are determined as minima of $\hat{U}_{\rm eff}$ for $X_Q^2 \geqslant 0$ and of ${\rm Re}\hat{U}_{\rm eff}$ for $X_Q^2 < 0$.

Errors arise from two sources. The first one are the imaginary parts in $\hat{U}_{\rm eff}$, when the saddle point is determined from the condition $\partial\hat{U}_{\rm eff}/\partial sad = 0$. For small temperatures, large effective masses and/or large values of n in Eq. (28), the contributions to the sum over n are so small that they reach the order of the numerical accuracy. The location of the saddle point becomes inaccurate under these conditions. Similarly, for small arguments (i.e., high temperatures, small values of X_Q) the approximations of the Weber functions Y_2 in the vicinity of their singularity at vanishing arguments become less reliable [24]. This explains why the error in sad^* increases with temperature, if simultaneously $|X_Q^2|^{1/2}$ becomes smaller.

The error Δsad^* is estimated from the ambiguity in finding the maximum of $\hat{U}_{\rm eff}$. It turns out that for low temperatures $\Delta sad^* \sim 0$, while it increases with temperature to $\Delta sad^* \sim \pm 0.006\ {\rm GeV}^2$ in the transition region in case of the chiral limit.

The uncertainty in the determination in sad^* leads to errors in the meson condensates, the effective masses X_Q, and the thermodynamic quantities ε, p, and s. In case of realistic masses, the errors $\Delta\langle\sigma_{0,8}\rangle$, which are induced in

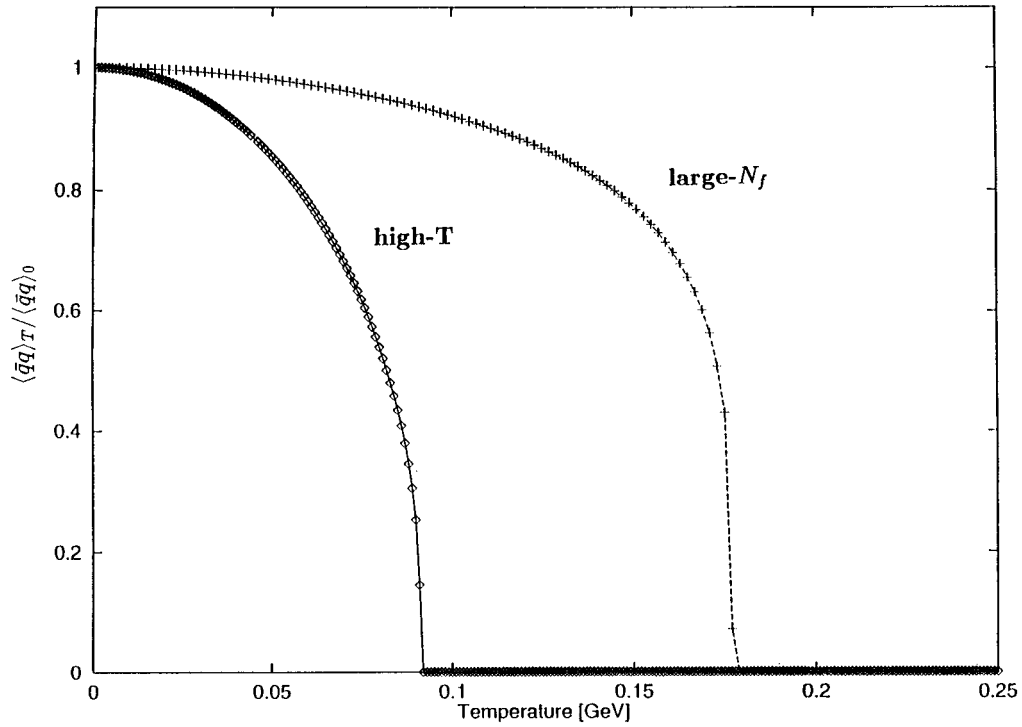

FIG. 1. Normalized light quark condensate $\langle\overline{qq}\rangle_T/\langle\overline{qq}\rangle_0$ as a function of temperature T in the high-temperature expansion (solid curve) and the numerical evaluation (dashed curve) of the large-N_f expansion. The condensate drops to zero at $T_c\sim 92$ MeV and 177 MeV, respectively.

$\langle\sigma_0\rangle,\langle\sigma_8\rangle$, are estimated as $\Delta\langle\sigma_{0,8}\rangle\leqslant 10^{-7}$ below $T\sim 50$ MeV, $\leqslant 10^{-4}$ below $T\sim 125$ MeV, $\leqslant 10^{-3}$ for $T\leqslant 165$ MeV, and of the order of 10^{-3} MeV in the transition region. After the crossover ($T\geqslant 197$ MeV) it stays $\sim 10^{-4}$.

A second source for errors in the condensates $\langle\sigma_0\rangle,\langle\sigma_8\rangle$ is the flat shape of the effective potential in the transition region; in particular, for external field strengths which only admit a rather weak first-order phase transition. We estimate $\Delta\langle\sigma_0\rangle(\simeq\Delta\langle\sigma_8\rangle)$ from plots of $\hat{U}_{\rm eff}(\sigma_0)$ in the SU(3) symmetric case. We find $\Delta\langle\sigma_0\rangle\simeq\pm 1.3$ MeV in the chiral limit and $\simeq\pm 4.3$ MeV for $\epsilon_0=2\times 10^{-4}$ or 2.5×10^{-4} GeV^3, cf. Fig. 3 of Sec. V.

When the meson condensates are converted to the quark condensates, additional errors enter because of the current quark masses. We use $\Delta m_{u,d}=\pm 1.45$ MeV [17].

Of particular interest are the errors in the entropy and energy densities s and ε in the crossover region, as they lead to an upper bound on a finite latent heat which cannot be excluded from our results. Their sizes can be traced back to errors in the effective masses X_Q. It is indicated in Fig. 5 of Sec. VI, where the curves refer to realistic meson masses.

From very different approximation schemes it is known that the region of a phase transition is particularly difficult to handle. Our difficulties in localizing the saddle point and calculating the condensates in the transition or crossover region are just a manifestation of that.

IV. THE CHIRAL LIMIT

From the renormalization group analysis of Pisarski and Wilczek [1] we expect a first-order chiral transition in the chiral limit. As mass input we choose $m_\pi^2=m_K^2=m_\eta^2=0$ for the pseudoscalar Goldstone bosons, $m_{\eta'}=850$ MeV, $m_{\sigma_{\eta'}}=800$ MeV, $f_\pi=94$ MeV. The mass of the σ meson should be treated as a parameter because of the uncertainty in the experimental identification. For the final parametrization we choose $m_{\sigma_\eta}=600$ MeV.

The tree-level parametrization of the Lagrangian (1) in the limit of vanishing ε_0 and ε_8 is then given by

$$\mu_0^2=5.96\times 10^{-2}\ \text{GeV}^2,$$

$$f_1=4.17,$$

$$f_2=4.48,$$

$$g=-1.81\ \text{GeV}. \tag{29}$$

The high-temperature expansion gives a first-order transition at $T_c=92\pm 1$ MeV, while the fully numerical evaluation leads to $T_c=177\pm 1$ MeV, cf. Fig. 1. This is in agreement with the general observation that the high-T expansion gives qualitatively correct results when it is extrapolated beyond its validity range, quantitatively it fails in precise predictions. The T_c value of the numerical calculation supports the estimate for the N_f dependence of T_c, which has been derived by Cleymans, Kocić, and Scadron [25] from a pion gas model without interactions as

$$T_c\sim 2f_\pi\sqrt{3N_f/(N_f^2-1)}\sim 200\ \text{MeV}. \tag{30}$$

The effective potential $\hat{U}_{\rm eff}$ is plagued with imaginary parts for all temperatures we have investigated, i.e., between 0 and 250 MeV. When we evaluate $\text{Re}\hat{U}_{\rm eff}$ according to Eq.

(28), we observe the same effect for higher values of the σ mass as it has been noticed by Goldberg [18]. Goldberg has calculated the effective potential of the SU(3)×SU(3) σ model in a mean-field approximation in the chiral limit. The oscillations in the potential became stronger for larger values of the σ-meson mass, which was used as input. In our case $\mathrm{Re}\hat{U}_{\mathrm{eff}}(\sigma_0)$ strongly fluctuates around the expected parabola if $m_\sigma \geqslant 1$ GeV. This explains our final parameter choice of $m_{\sigma_\eta}=600$ MeV. The approximation of $\mathrm{Re}\hat{U}_{\mathrm{eff}}$ according to Eq. (28) by a finite series of Weber functions ($n \leqslant 25$) loses its validity if the argument of Y_2 becomes too large because of m_σ^2.

For the barrier height between the coexisting minima of the potential we find 0.14×10^{-3} GeV/fm^3. The barrier height may be regarded as a measure for the strength of the transition. It determines the tunneling rate between coexisting phases in the transition region. The barrier height is clearly smaller than the value of Frei and Patkós [19], who found 0.36 GeV/fm^3 in the same model, but without inclusion of the $n\neq0$-Matsubara frequencies. The higher barrier goes along with a large value for the interface tension α between the coexisting chirally broken and symmetric phases at T_c, α has been estimated as [(40–50) MeV]^3 [19]. More recent lattice results indicate that such a large value is not likely for QCD [26].

V. THE CRITICAL TRANSITION LINE

The critical transition line in an $(m_\pi, m_K, \ldots)$ diagram consists of pseudoscalar meson masses for which the first-order chiral transition becomes of second-order and turns into a crossover phenomenon for meson masses exceeding the so-called critical values. We will determine three such critical points. The critical points are characterized by their external field strengths $\varepsilon_0, \varepsilon_8$. The first point corresponds to an SU(3) symmetric case, where $\varepsilon_8=0$, $m_u=m_d=m_s\neq0$, and $m_\pi=m_K=m_\eta\neq0$. Since $\langle\sigma_8\rangle=0$ for all temperatures, the numerics considerably simplify compared to the general case with $\varepsilon_0\neq0\neq\varepsilon_8$. For the second critical point we choose $\varepsilon_0=-0.77\varepsilon_8$. This ratio is identical to $\varepsilon_0/\varepsilon_8$ for the mass point with realistic meson masses, where $m_s/\hat{m}=18.2$, cf. Sec. II. The third point is characterized by $\varepsilon_0=(2\alpha/\beta)\varepsilon_8$. It is chosen such that $m_s=0$, $m_{u,d}\neq0$. Before we present our results for the critical field strengths in the large-N_f expansion, we calculate $\varepsilon_0^{\mathrm{crit}}$, $\varepsilon_8^{\mathrm{crit}}$ in a mean-field approximation.

A. Critical meson masses in a mean-field approximation

Recently, Gavin, Gocksch and Pisarski [15] have calculated a set of critical quark masses in the linear SU(3)×SU(3) σ model. The calculation has been performed in a mean-field approximation. Since we use a different tree-level parametrization of the σ model, we have performed the mean-field calculation for our parameter choice. Here, we summarize the main steps for the simpler SU(3) symmetric case.

The SU(3) symmetric case. In mean field we have to deal with the classical part of the potential U_{class}, which follows from the Lagrangian (1) for a constant background field $\sigma_0=\overline{\sigma_0}(\overline{\sigma_8}=0)$, and $\epsilon_8=0$. We have

$$U_{\mathrm{class}}(\sigma_0)=-\frac{1}{2}\mu_0^2\sigma_0^2+\frac{2}{3\sqrt{3}}g\sigma_0^3+\left(f_1+\frac{f_2}{3}\right)\sigma_0^4-\varepsilon_0\sigma_0. \tag{31}$$

This form is familiar from Landau's free energy functional in terms of an order parameter field. One of its applications is a description of the phase structure for a liquid-gas transition. For $\varepsilon_0=0$ the system has a first-order transition from the liquid to the gas phase. The transition stays first order, until the external field (the pressure in case of a liquid-gas system) is increased to a critical value $\varepsilon_0^{\mathrm{crit}}$, where it becomes of second order. For values of $\varepsilon_0>\varepsilon_0^{\mathrm{crit}}$, the transition is washed out and turns into a crossover phenomenon.

In mean field the effect of a finite (and strictly speaking high) temperature is reduced to a renormalization of the mass parameter term, i.e., the coefficient of the quadratic term in the Lagrangian. Thus, the finite temperature effects can be mimicked by tuning μ_0^2 while keeping the other couplings in the Lagrangian (f_1, f_2, g) fixed. The potential can be Taylor expanded around its true minimum σ_0^{min} (which is different from zero in the symmetry broken phase); in particular, it can be expanded around the ''critical'' $\sigma_0^{\mathrm{min}}\equiv\sigma_0^{\mathrm{crit}}$ for the critical field strength $\varepsilon_0^{\mathrm{crit}}$. In the ''critical'' case U_{class} starts with a term quartic in $(\sigma_0-\sigma_0^{\mathrm{crit}})$. From the vanishing of the first three coefficients we obtain the critical parameters as follows. The vanishing of the third derivative of U_{class} with respect to σ_0 at $\sigma_0=\sigma_0^{\mathrm{crit}}$ leads to

$$\sigma_0^{\mathrm{crit}}=\frac{-g}{\sqrt{3}\times6(f_1+f_2/3)}=3.1\times10^{-2}\ \mathrm{GeV}. \tag{32}$$

The second derivative $\partial^2U_{\mathrm{class}}/\partial\sigma_0^2$ at σ_0^{crit} is the coefficient of the quadratic fluctuations $(\sigma_0-\sigma_0^{\mathrm{crit}})^2$ around σ_0^{crit} with the meaning of $m_{\sigma_{\eta'}}^2$. This is the critical mass, which goes to zero when the second-order transition is approached. It is easily checked that the other meson masses remain finite for the same set of critical parameters. The vanishing of $m_{\sigma_{\eta'}}^2$ at criticality implies for the critical value of μ_0^2

$$\mu_0^{2\,\mathrm{crit}}=\frac{-g^2}{9(f_1+f_2/3)}=-6.44\times10^{-2}\ \mathrm{GeV}^2. \tag{33}$$

Finally, the extremum condition for σ_0^{crit} determines $\varepsilon_0^{\mathrm{crit}}$ as

$$\varepsilon_0^{\mathrm{crit}}=-\frac{1}{27\times6\times\sqrt{3}}\frac{g^3}{(f_1+f_2/3)^2}=6.6\times10^{-4}\ \mathrm{GeV}^3. \tag{34}$$

The value for $\varepsilon_0^{\mathrm{crit}}=6.6\times10^{-4}$ GeV^3 ($\varepsilon_8^{\mathrm{crit}}=0$) leads to a pseudoscalar octet mass of $m_\pi=m_K=m_\eta=146$ MeV and a current quark mass of $m_u=m_d=m_s=1.9$ MeV.

One should keep in mind that the tree-level parametrization of the SU(3)×SU(3) σ model is arbitrary to some extent. If we would choose $g=-1.39$ GeV, $f_1=5.3$, $f_2=0.93$ with $m_{\sigma_\eta}=600$ MeV (the values which have been used in [8] for the tree-level parametrization), $\varepsilon_0^{\mathrm{crit}}$ turns out as 3×10^{-4} GeV^3 or $m_{u,d,s}\simeq0.9$ MeV leading to $\langle m_P\rangle=115$ MeV. For the same parameter choice, but

$f_1=2.35$ and $m_{\sigma_\eta}=950$ MeV, $\varepsilon_0^{\rm crit}$ comes out as 1.3×10^{-3} GeV^3. The same tendency has been observed in [15]. An increase of the input mass m_{σ_η} shifts the critical field strength to larger values (reducing the discrepancy to the lattice result). The parameter choice which has been used in [16] leads to $\varepsilon_0^{\rm crit}=4\times10^{-4}$ GeV^3. Gavin, Gocksch, and Pisarski [15] obtain for the corresponding critical field strength in the SU(3) symmetric case $h_0^{\rm crit}=1.6\times10^{-4}$ GeV^3. Because of their different parametrization it is only of the same order of magnitude as ours. Thus, we estimate the error in the mean-field calculation as $\Delta\epsilon_0^{\rm crit}=\pm5\times10^{-4}$ GeV^3. The induced error in the pseudoscalar meson masses comes out as large as ≈127 MeV, in the current light quark mass it is $\leqslant1.4$ MeV.

The general case of $\varepsilon_0\neq0$, $\varepsilon_8\neq0$. For nonvanishing ε_0 and ε_8 $U_{\rm class}$ is given by Eq. (19). Again, we have to determine the critical parameter μ_0^2 to simulate a finite temperature, the critical minima values $\sigma_0^{\rm crit},\sigma_8^{\rm crit}$ of $U_{\rm class}$, and the critical field strengths $\varepsilon_0^{\rm crit},\varepsilon_8^{\rm crit}$. We use the conditions

$$\partial U_{\rm class}(\sigma_0,\sigma_8)/\partial\sigma_0|_{\rm crit}=0, \tag{35}$$

$$\partial U_{\rm class}(\sigma_0,\sigma_8)/\partial\sigma_8|_{\rm crit}=0, \tag{36}$$

$$m^2_{\sigma_{\eta'}}|_{\rm crit}=0, \tag{37}$$

$$\varepsilon_0^{\rm crit}/\varepsilon_8^{\rm crit}+0.77|_{\rm crit}=0, \tag{38}$$

$$\partial^3 U_{\rm class}(\sigma_0,\sigma_8)/\partial r^3|_{\rm crit}=0\,. \tag{39}$$

The five conditions are postulated at criticality (abbreviated as $|_{\rm crit}$), i.e., for the set of critical parameters $\sigma_0^{\rm crit}$, $\sigma_8^{\rm crit}$, $\varepsilon_0^{\rm crit}$, $\varepsilon_8^{\rm crit}$, $\mu_0^{2\,\rm crit}$. The first three equations are obvious generalizations of the SU(3) symmetric case. Equation (38) is just one possible choice saying that we keep the mass splitting of realistic (pseudo)scalar meson masses fixed in the tuning to the critical transition line. Equation (39) generalizes $\partial^3 U_{\rm class}(\sigma_0)/\partial\sigma_0^3|_{\rm crit}=0$ of the one-dimensional case. More precisely, it postulates that the directional derivative in the radial direction r in (σ_0,σ_8) space (i.e., in the direction of $m^2_{\sigma_{\eta'}}=0$) should vanish to exclude the occurrence of a first-order transition. Equations (35)–(39) are solved numerically. We find

$$\sigma_0^{\rm crit}=3.7\times10^{-2}\ \text{GeV},\quad \sigma_8^{\rm crit}=-5.0\times10^{-3}\ \text{GeV}, \tag{40}$$

$$\mu_0^{2\,\rm crit}=-6.4\times10^{-2}\ \text{GeV}^2, \tag{41}$$

$$\varepsilon_0^{\rm crit}=7.0\times10^{-4}\ \text{GeV}^3,\quad \varepsilon_8^{\rm crit}=-9.1\times10^{-4}\ \text{GeV}^3, \tag{42}$$

or $m_s=5.4$ MeV, $\hat m=0.3$ MeV, while the average pseudoscalar meson mass $\langle m_P\rangle=120$ MeV. The values for $\varepsilon_{0,8}^{\rm crit}$ are compatible with the results of [15], who find for the critical field strengths $h_0^{\rm crit}=(62\ \text{MeV})^3, h_8^{\rm crit}=(60.4\ \text{MeV})^3$, if one keeps in mind the different tree-level parametrization. For example, $m_s/m_{u,d}=32$ in [15], while $m_s/m_{u,d}=18.2$ in our case.

The case of $m_s=0$ *or* $\varepsilon_0/\varepsilon_8=2\alpha/\beta$. If we replace 0.77 in Eq. (38) by $-2\alpha/\beta=-1.31$ corresponding to $m_s=0$, $m_{u,d}\neq0$, we obtain, from Eqs. (35)–(39),

$$\sigma_0^{\rm crit}=3.4\times10^{-2}\ \text{GeV},\quad \sigma_8^{\rm crit}=2.9\times10^{-3}\ \text{GeV} \tag{43}$$

$$\mu_0^{2\,\rm crit}=-6.4\times10^{-2}\ \text{GeV}^2 \tag{44}$$

$$\varepsilon_0^{\rm crit}=6.7\times10^{-4}\ \text{GeV}^3,\quad \varepsilon_8^{\rm crit}=5.14\times10^{-4}\ \text{GeV}^3, \tag{45}$$

or $\hat m=2.9$ MeV and $\langle m_P\rangle=137.2$ MeV. Note that the condition $m_s=0$ implies the same sign for $\varepsilon_0^{\rm crit}$ and $\varepsilon_8^{\rm crit}$ because of the same sign for the constants α and β. Hence, the ''critical'' condensates $\sigma_{0,8}^{\rm crit}$ come out with equal sign in contrast with the realistic mass case.

In the following we will compare the mean-field values for $\varepsilon_{0,8}^{\rm crit}$ with the large-N_f results.

B. Critical meson masses in the large-N_f expansion

The SU(3) symmetric case. When $\varepsilon_8=0$ and ε_0 is slowly increased from 0 to $\sim2.5\times10^{-4}$ GeV^3, we observe a weakening of the first-order transition as is seen in Fig. 2. For the critical field strength we find

$$\varepsilon_0^{\rm crit}\leqslant(3\pm0.5)\times10^{-4}\ \text{GeV}^3. \tag{46}$$

The value for $\varepsilon_0^{\rm crit}$ induces an upper bound on the pseudoscalar meson mass of 51 MeV or on the quark masses of $m_{u,d}^{\rm crit}=m_s^{\rm crit}\leqslant0.9\pm0.14$ MeV, such that

$$m_{u,d,s}^{\rm crit}/m_{u,d,s}\leqslant0.08\pm0.01. \tag{47}$$

Within the errors the result for $\varepsilon_0^{\rm crit}$ is of the same order of magnitude as the mean-field value. The uncertainty in our result is $\Delta\varepsilon_0^{\rm crit}\leqslant0.5\times10^{-4}$ GeV^3. For $\varepsilon_0=2.5\times10^{-4}$ GeV^3 the transition could be clearly identified as first order from the $\langle\overline{qq}\rangle_T/\langle\overline{qq}\rangle_0(T)$ curves. For $\varepsilon_0=3\times10^{-4}$ GeV^3 it is a crossover. We could have further improved the accuracy of $\varepsilon_0^{\rm crit}$ by measuring data for $\langle\overline{qq}\rangle_T(T)$ in the intermediate ε_0 range. On the other hand, such an improvement is limited by the well-known fact that it is, in general, hard to disentangle a very weak first-order transition from a rapid crossover phenomenon.

The weakening of the first-order transition is also revealed in the barrier height of the effective potential between the coexisting minima at T_c. The barrier decreases from 1.4×10^{-4} GeV/fm^3 in the chiral limit to 2.1×10^{-6} GeV/fm^3 for $\varepsilon_0=2.0\times10^{-4}$ GeV^3, $\varepsilon_8=0$ GeV^3, the largest value for which a first-order transition could be identified from the shape of the effective potential, cf. Fig. 3. A comparison between Figs. 2 and 3 shows the ambiguity in identifying a very weak first-order transition. Figure 2 suggests a weak first-order transition for $\varepsilon_0=2.5\times10^{-4}$ GeV^3 with $T_c\sim181$ MeV, but no barrier is visible between the two coexisting condensate values at the same temperature and the same ε_0 value in Fig. 3. Accordingly, a precise determination of T_c is hard in case of a weak first-order transition such that we estimate the error in T_c as $\Delta T_c=\pm2$ MeV. Figure 3 also admits an estimate of the error in finding $\langle\sigma_{0,8}\rangle$ in the transition or crossover region if the effective potential is very

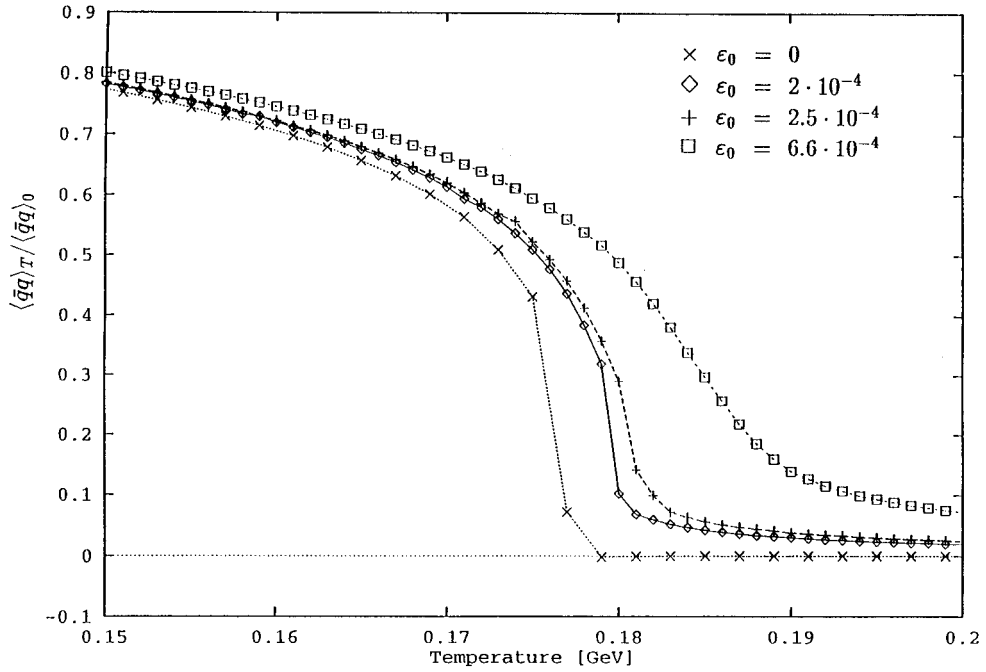

FIG. 2. The light quark condensate normalized to its value at zero temperature $\langle \overline{qq} \rangle_T / \langle \overline{qq} \rangle_0$ as a function of T in the SU(3) symmetric case. The weakening of the first-order transition is obvious, when ε_0 GeV^3 is varied between $\varepsilon_0 = 0(\times)$, $2\times10^{-4}(\diamond)$, $2.5\times10^{-4}(+)$, and $6.6\times10^{-4}(\square)$.

flat, which we have mentioned in Sec. III. In the chiral limit we have $\Delta\langle\sigma_0\rangle \sim 1.3\times10^{-3}$ GeV, for $\varepsilon_0 = 2\times10^{-4}$ and for $\varepsilon_0 = 2.5\times10^{-4}$ GeV^3 the error is estimated as 4.3×10^{-3} GeV. Later, we assume $\Delta\langle\sigma_0\rangle \sim \Delta\langle\sigma_8\rangle$.

$T_c(m)$ dependence in the SU(3) *symmetric case.* For simplicity, we restrict the study of the mass dependence of T_c in the first-order transition region to the SU(3) symmetric case. Table I shows an increase of T_c with the current quark mass $\hat{m}$. For realistic mass values of $m_\pi = 129.3$ MeV, $m_K = 490.7$ MeV, $m_\eta = 544.7$ MeV (not listed in Table I), the rapid crossover sets in at $T \sim 181.5$ MeV and becomes slow at ~ 192.6 MeV. We associate a critical temperature ''T_c'' $\sim 187 \pm 0.5$ MeV to this crossover phenomenon for comparison with extrapolated values of T_c in chiral perturbation theory (in our case T_c is localized as the point of inflection in the crossover curve). Thus, T_c has increased by 5.3% compared to the chiral limit. This result is in agreement with the estimate of Leutwyler [27], who predicts $\Delta T_c / T_c \sim 5\%$ if realistic pion masses are substituted for the chiral limit with $m_\pi = 0$. When the critical temperature is extrapolated in the framework of chiral perturbation theory, the inclusion of finite quark masses delays the melting of $\langle \overline{qq} \rangle$ by $\Delta T \sim 20$ MeV [4], while the inclusion of heavier mesons in a dilute gas approximation has the opposite effect. At finite quark

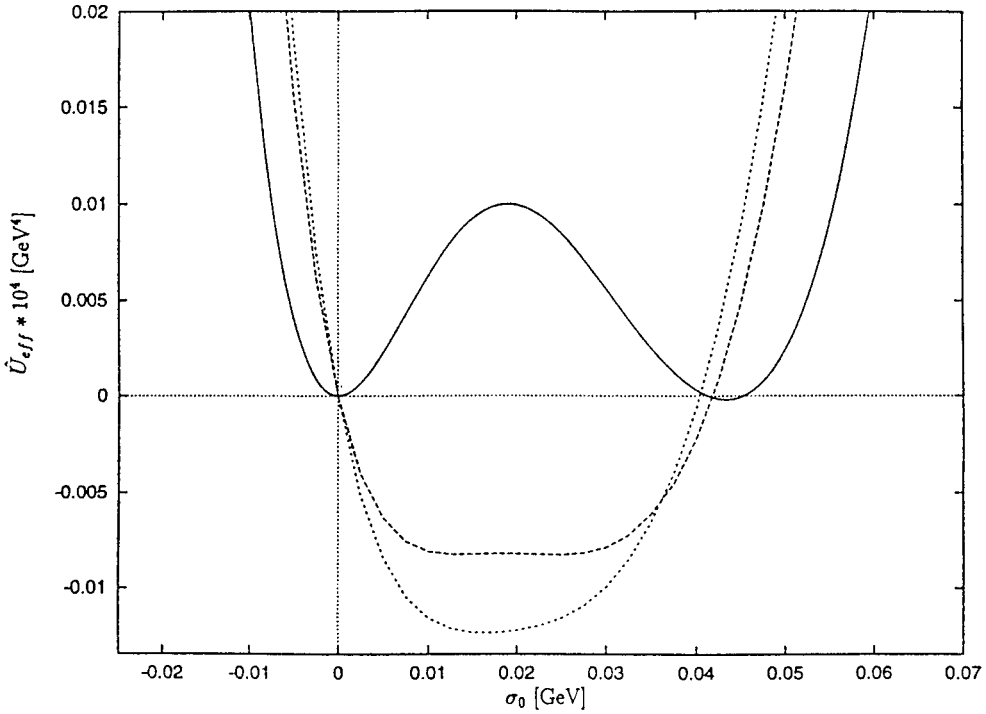

FIG. 3. Decrease of the barrier height of the effective potential $\hat{U}_{\text{eff}}$ for $\varepsilon_0 = 0$ at $T \sim 176$ MeV (solid curve), $\varepsilon_0 = 2\times10^{-4}$ GeV^3 at $T \sim 180$ MeV^3 (dashed curve), $\varepsilon_0 = 2.5\times10^{-4}$ GeV^3 for $T \sim 181$ [MeV] (determined from the corresponding condensate curve of Fig. 2) (dotted curve) in the SU(3) symmetric case.

TABLE I. The critical temperature T_c as a function of the average light quark mass $\hat{m}$ in the SU(3) symmetric case.

$\hat{m}$ [MeV]	0	0.29	0.57	0.71
T_c [MeV]	177	178.5	179.4	180.4

masses it accelerates the melting from $T_c \sim 240$ MeV–190 MeV. The delay in the melting because of finite quark masses is intimately related to the size of the latent heat. The relation is revealed in the derivation of a Clausius-Clapeyron equation for QCD, cf. [27]. Thus, the $T_c(m)$ dependence is conclusive for the strength of a first-order chiral transition.

The case of realistic mass splitting, $\varepsilon_0^{\rm crit}/\varepsilon_8^{\rm crit}=0.77$. For the realistic mass splitting induced by $m_s/m_{u,d}=18.2$ we find, for the critical field strengths in large N_f,

$$\varepsilon_0^{\rm crit} \leqslant (7\pm 2)\times 10^{-3}\,{\rm GeV}^3,$$

$$\varepsilon_8^{\rm crit} \geqslant (-9.09\pm 2.6)\times 10^{-3}\ \ {\rm GeV}^3, \tag{48}$$

corresponding to an average pseudoscalar octet mass of $\langle m_P\rangle \leqslant 203$ MeV. The critical values for the current quark masses are $m_{u,d}^{\rm crit} \leqslant 2.96\pm 0.85$ MeV and $m_s^{\rm crit} \leqslant 54\pm 15.4$ MeV. The reason why we give an upper/lower bound on $\varepsilon_{0,8}^{\rm crit}$ rather than precise values for the first-order transition boundary is the same as in the SU(3)-symmetric case. The bound on $\varepsilon_{0,8}^{\rm crit}$ could still be improved by measuring data between $\varepsilon_0=4\times 10^{-3}$ GeV^3, $\varepsilon_8=-5.2\times 10^{-3}$ GeV^3, where the transition is still of first order, and $\varepsilon_0^{\rm crit}$, $\varepsilon_8^{\rm crit}$ from Eq. (48). It should be remarked that, because of the small gap in the condensate, only a rather fine resolution of the $\langle \overline{qq}\rangle/\langle \overline{qq}\rangle_0(T)$ curve in steps of $\Delta T \leqslant 0.1$ MeV has revealed the true first-order nature of the transition for $\varepsilon_0=5\times 10^{-3}$ and $\varepsilon_8=-6.5\times 10^{-3}$ GeV^3.

Thus we see that also in a large-N_f expansion tiny values for the quark masses are sufficient to weaken the chiral transition and turn it finally into a crossover phenomenon. Similarly, tiny current quark masses are sufficient to eliminate the chiral transition in an SU(3) Nambu–Jona-Lasinio model as a function of temperature and nuclear density [28].

The large-N_f results for $\varepsilon_{0,8}^{\rm crit}$ are clearly above the mean-field values of Eq. (42). The result is plausible, as our saddle-point approximation goes beyond the mean-field calculation. The leading term in a $1/N_f$ expansion corresponds to the summation of a class of diagrams, called ''super-daisies'' [29]. Super daisies have been summed up by Dolan and Jackiw [21] to circumvent the IR-divergence problem in an N-component ϕ^4 theory. Our application of the $1/N_F$ method to the linear σ model has been similar in spirit. Certainly we cannot claim that the fluctuations we have included so far are representative for all fluctuations. In fact, the classical cubic term of our potential may still dominate the driving mechanism for the first-order transition below the critical field strengths. Only the lattice calculation includes all fluctuations by simulating the full partition function at once (at least in principle). This may explain the remaining discrepancy between the large-N_f ratio and the lattice result for $m_{u,d}^{\rm crit}/m_{u,d}$.

The next question which arises in a comparison with the mean-field calculation concerns the critical renormalized masses, which should vanish for the critical field strengths at a second-order transition. In the mean-field calculation $m_{\sigma_{\eta'}}^2$ vanishes by construction for the set of critical parameters, and it is easily checked that $m_{\sigma_{\eta'}}$ is the only mass that vanishes at criticality. Our value for $m_{\sigma_{\eta'}}=749.5$ MeV is the tree-level input mass at zero temperature, which needs not vanish. The effective masses X_Q are temperature dependent. It is not obvious to us that one of these masses should induce an infinite correlation length as T approaches T_c. A careful renormalization prescription should be imposed to identify the renormalized mass(es) that goes(go) to zero for critical external fields. It would further allow an identification of the universality class of the SU(3)×SU(3) linear σ model for critical parameters $\mu_0^2, f_1, f_2, g, \varepsilon_0, \varepsilon_8$. We will investigate these questions in a forthcoming work.

Critical meson masses for $m_s=0$. Here, the large-N_f results are even somewhat smaller than the mean-field results [cf. Eqs. (45)]. We find

$$\varepsilon_0^{\rm crit} \leqslant (4\pm 1)\times 10^{-4}\ \ {\rm GeV}^3,$$

$$\varepsilon_8^{\rm crit} \leqslant (3.06\pm 0.76)\times 10^{-4}\ \ {\rm GeV}^3. \tag{49}$$

The associated average pseudoscalar octet mass is $\langle m_P\rangle \leqslant 57.2\pm 28.8$ MeV, and $m_{u,d} \leqslant 1.7\pm 0.4$ MeV, while $m_s=0$ by construction.

The Columbia plot has suggested a concave shape of the first order transition boundary. The three critical masses in mean field are compatible with such a shape in an (m_π, m_K) or an $(\hat{m}, m_s)$ diagram, although one should keep in mind the large error bars because of the ambiguity in the tree-level parametrization of the σ model, and the sensitive dependence of the boundary on the $\sigma_{\eta^{(\prime)}}$-mass input. The three critical masses in large N_f do not confirm the conjectural concave shape. Only for a realistic ratio of $\varepsilon_0/\varepsilon_8$, the large-$N_f$ result lies clearly above the mean-field value for the critical masses. The errors here are at least as large as in the mean-field case, although they could have been further reduced.

In the next section we will see the change in the crossover behavior, as $\varepsilon_0, \varepsilon_8$ are further increased to induce realistic mass values.

VI. THE REALISTIC MASS POINT

If we use for μ_0^2, f_1, f_2, g the values of the chiral limit and choose $\varepsilon_0=0.0265$ GeV^3, $\varepsilon_8=-0.0345$ GeV^3, we find (pseudo)scalar meson masses which are listed in Table II. A comparison to the experimental values shows reasonable agreement for the pseudoscalar mesons. Therefore, we call this point the ''realistic'' mass point. The experimental values which are associated to the scalar meson masses depend on the identification, which is indicated in a separate row of Table II. The mass splitting between K_0^* and a_0 comes out too small in our case. We could have further optimized our choice of ε_0 and ε_8 to improve the agreement with the experimental mass values, but such an optimization should be inconsequential for our results.

Crossover in the condensates. The crossover behavior for the normalized light and strange quark condensates is dis-

TABLE II. Tree-level parametrization of the SU(3)×SU(3) linear σ model for the realistic mass point.

Input

μ_0^2 GeV^2	f_1	f_2	g MeV	f_π MeV	ε_0 GeV^3	ε_8 GeV^3
5.96×10^{-2}	4.17	4.48	-1812.0	94	0.0265	-0.0345

Output (all masses are understood in units of MeV)

	m_π	m_K	m_η	$m_{\eta'}$	m_{σ_π}	m_{σ_K}	m_{σ_η}	$m_{\sigma_{\eta'}}$
Real. Mass Point	129.3	490.7	544.7	1045.5	1011.6	1031.2	1198.0	749.5
Expt. Mass Values	138.0	495.7	547.5	957.8	980 if $\sigma_\pi \equiv a_0$	1322.0 if $\sigma_K \equiv K_0^*$	1476.0 if $\sigma_\eta \equiv f_0(1476)$	975 if $\sigma_{\eta'} \equiv f_0(975)$

played in Fig. 4. The rapid crossover leads to a decrease of $\sim$50% of the condensate at zero temperature $\langle\overline{qq}\rangle_0$ in $\langle\overline{qq}\rangle_T$ over a temperature interval $\Delta T\sim10$ MeV, while $\langle\overline{ss}\rangle_T$ stays remarkably constant up to $T\sim197$ MeV, where it starts to decrease rather slowly. The physical reason is obvious. It is harder to excite mesons with strange quarks than those with light quarks. The same qualitative behavior of $\langle\overline{ss}\rangle_T$ has been noticed by Hatsuda and Kunihiro [30] in a $U_{N_f}(3)$ version of the Nambu–Jona-Lasinio (NJL) model. Also, the location of the crossover region in the NJL model is around $T\sim200$ MeV.

We have indicated the error bars only in the crossover region where they are largest. When the errors in the current quark masses are added, which enter Eq. (12), we obtain $\Delta\langle\overline{qq}\rangle\sim3.1\times10^{-3}$ GeV^3, $\Delta\langle\overline{ss}\rangle\sim6.7\times10^{-3}$ GeV^3 at $T=180$ MeV in the transition region. In Fig. 4 we have indicated only the numerical errors, the contribution from the current quark masses has been left out. Compared to critical meson masses ($\varepsilon_0^{\rm crit}=7\times10^{-3}$ GeV^3, $\varepsilon_8^{\rm crit}=-9.1\times10^{-3}$ GeV^3), the crossover happens over a larger temperature interval. We find $\Delta[\langle\overline{qq}\rangle_T/\langle\overline{qq}\rangle_0]^{\rm real}/\Delta[\langle\overline{qq}\rangle_T/\langle\overline{qq}\rangle_0]^{\rm crit}\sim52\%$ if $\Delta[\langle\overline{qq}\rangle_T/\langle\overline{qq}\rangle_0]$ denotes the normalized condensate change per 1 MeV temperature interval in the rapid part of the crossover region. Nevertheless, the crossover in the quark condensate $\langle\overline{qq}\rangle$ seems to be sharp even for realistic masses. Such a rapid change may lead to visible changes in hadron

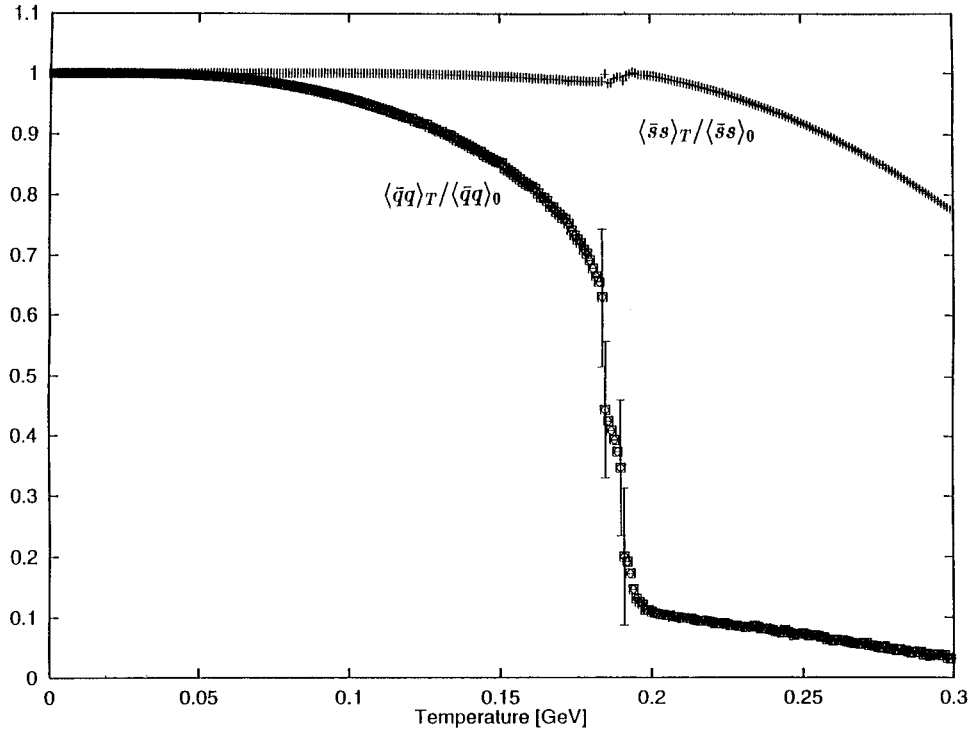

FIG. 4. Light ($\langle\overline{qq}\rangle$) and strange ($\langle\overline{ss}\rangle$) quark condensates normalized to their corresponding values at zero temperature as a function of temperature. The crossover behavior is most rapid between $181.5\leqslant T\leqslant192.6$ MeV.

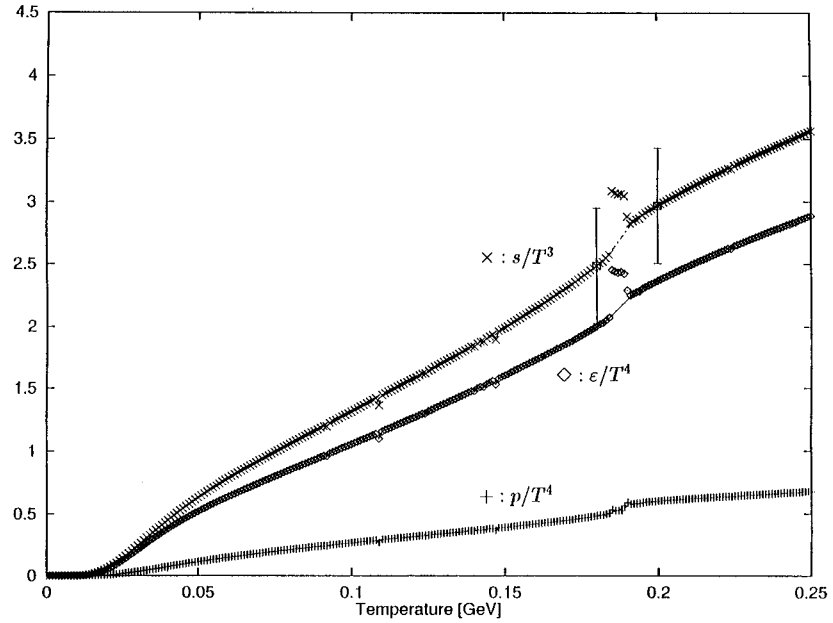

FIG. 5. Entropy density s over T^3, energy density ε over T^4, and pressure p over T^4 in the large-N_f expansion for the realistic mass point. Errors are only indicated for s/T^3.

masses, depending on temperature and condensates. It could be manifest in hadronic or dilepton spectra in heavy-ion experiments.

Thermodynamics. Further characteristics of the crossover phenomenon are the variations in the energy and entropy densities over the temperature interval in the crossover region. At this place one should recall the very definition of a first-order phase transition. At the transition point *at least one* of the first derivatives of a suitable thermodynamic potential should behave discontinuously in the infinite volume limit. Thus, a crossover in the condensates, in general, does not exclude a finite gap in the energy or entropy densities. In Fig. 5 we have plotted s/T^3, ε/T^4, and p/T^4. The data points are strongly fluctuating within a range, which is indicated by the error bars for the entropy curve. The errors for the energy density are of similar size. Errors enter via the effective masses X_Q^2, which depend on $\langle\sigma_0\rangle$, $\langle\sigma_8\rangle$ and sad^*. We have used for $\Delta\langle\sigma_0\rangle\sim(1.0--3.0)\times10^{-3}$ GeV $=\Delta\langle\sigma_8\rangle$ and $\Delta sad^*\sim0.11$ GeV^2 in the crossover region between $T=182-193$ MeV. The pressure behaves continuously as a function of T if it is calculated as $p=(-\hat{U}_{\rm eff})$. There is only a change of slope in the critical crossover region. A direct calculation of p with an integral expression pretends a discontinuity. The p/T^4 curve in Fig. 5 is obtained from $(p=-\hat{U}_{\rm eff})$. As change in the entropy density we find from the actually measured data

$$T\Delta s\leqslant 0.16\pm0.02\ \ \text{GeV/fm}^3 \tag{50}$$

in a temperature interval $181.5\leqslant T\leqslant192.6$ MeV, where $T\Delta s$ is calculated as $T_2s(T_2)-T_1s(T_1)$. As rapid change in the energy density we find

$$\Delta\varepsilon\leqslant 0.13\pm0.02\ \ \text{GeV/fm}^3 \tag{51}$$

or $\Delta\varepsilon/T_c^4\equiv\varepsilon(T_2=192.6\ \text{MeV})/T_2^4-\varepsilon(T_1=181.5\ \text{MeV})/T_1^4=0.29$ over the same temperature range. For comparison we mention that the gap in the gluonic energy density $\Delta\varepsilon_g$ in a pure SU(3) gauge theory leads to [31,32]

$$\frac{\Delta\varepsilon_g}{T_c^4}=\begin{cases}2.44\pm0.24 & \text{for } N_\tau=4,\\ 1.80\pm0.18 & \text{for } N_\tau=6,\end{cases} \tag{52}$$

where N_τ refers to the lattice extension in time direction. These values are by an order of magnitude larger than our value for the mesonic contribution $\Delta\varepsilon/T_c^4\sim0.29$, defined as indicated above. The decrease of $\Delta\varepsilon_g/T_c^4$ under an increase of the time extension N_τ indicates strong finite-size effects. Going to larger lattices this tendency may continue and further reduce the latent heat, but it also gives us a warning. The contribution of $\Delta\varepsilon_g$ to the total energy gap may be superimposed on the slow change of ε that we have found in the crossover region and make the crossover in the total energy density more rapid. If the size of the errors in sad^*, $\langle\sigma_0\rangle$, $\langle\sigma_8\rangle$ is assumed as above, s could vary in the crossover region between T_1 and T_2 such as

$$s(T_2)T_2-s(T_1)T_1\leqslant0.18\pm0.02\ \ \text{GeV/fm}^3, \tag{53}$$

where the resulting error $\Delta(s/T^3)$ has been estimated as ±0.46, cf. Fig. 5. In an infinitesimally small temperature interval such a gap in s would lead to a finite latent heat ΔL of $\leqslant0.2$ GeV/fm^3. Thus, Eq. (53) gives a loose upper bound on the latent heat which could be compatible with our data because of the large errors in the crossover region. Note that $\Delta L=0.2$ GeV/fm^3 is only 10% of the value, which is predicted from the bag model equation of state. The bound comes out even smaller if the error of 0.46 is interpreted as $\Delta s/T_c^3$ with ''T_c'' = 187 MeV. It leads to $\Delta L=T_c\Delta s\leqslant0.074$ GeV/fm^3. Both bounds are even smaller than Leutwyler's value of 0.4 GeV/fm^3 for $T\Delta s$, [27] which has been obtained from a Clausius-Clapeyron equation in the framework of chiral perturbation theory. The small size of the latent heat is finally a consequence of the sensitivity of T_c to the inclusion of finite quark masses.

Clausius-Clapeyron equations relate the discontinuities in the condensate and the entropy or energy densities. Although they strictly apply to first-order transitions in the form of

Eqs. (54) and (55) below [27], we have tested the relations for the above crossover phenomenon in two forms. The first one is

$$\mathrm{disc}\langle\overline{qq}\rangle_T|_{\mathrm{RC}}=\left.\frac{\Delta T_c}{\Delta\hat{m}}\right|_{\mathrm{RC}}\mathrm{discs}|_{\mathrm{RC}}, \tag{54}$$

where $\mathrm{disc}\ldots|_{\mathrm{RC}}$ refers to the rapid change (''discontinuity'') in the crossover region and ΔT_c is the change in ''T_c'' under a variation $\Delta\hat{m}$ of the current light quark masses. The second version is

$$\frac{\Delta T_c}{T_c}|_{\mathrm{RC}}=\left|\frac{\mathrm{disc}\langle\overline{qq}\rangle_T}{\langle\overline{qq}\rangle_0}\right|_{\mathrm{RC}}\left|\frac{f_\pi^2 m_\pi^2}{\Delta\varepsilon}\right|_{\mathrm{RC}}. \tag{55}$$

In Eq. (54) we use $\Delta T_c/\Delta\hat{m}=(0.187-0.178)/0.011$, $\Delta s=0.0061\ \mathrm{GeV}^3$, $\mathrm{disc}\langle\overline{qq}\rangle_T=0.5\times(0.22)^3\ \mathrm{GeV}^3$, and obtain 0.005 for both sides of Eq. (54). In Eq. (55) we have ΔT_c as above, $T_c=178$ MeV, $\mathrm{disc}\langle\overline{qq}\rangle_T/\langle\overline{qq}\rangle_0=\langle\overline{qq}\rangle_{T_1}/\langle\overline{qq}\rangle_0-\langle\overline{qq}\rangle_{T_2}/\langle\overline{qq}\rangle_0=0.5$, $f_\pi=94$ MeV, $m_\pi=129$ MeV (the value of our realistic mass point), and $\Delta\varepsilon=0.001\ \mathrm{GeV}^4$. This way, we obtain for the right-hand side (RHS) 7% and for the LHS 5 % in Eq. (55). The agreement of the order of magnitude on both sides indicates that the crossover phenomenon is still rapid enough to satisfy analogous relations to a first-order transition in the strict sense.

We have further analyzed the contribution of the strange (pseudo)scalar mesons K and σ_K to the total energy density ε. Their contribution can be completely neglected below 40 MeV. It increases with temperature to $\sim 31\%$ in the crossover region around $T=187$ MeV. After the crossover the tendency continues, but is no longer conclusive for us because of the lack of quark degrees of freedom in the chiral symmetric phase.

The strangeness content of the plasma has been estimated in a lattice simulation [33] with light quark masses of $m_u/T=m_d/T=0.05$ and one heavier quark mass of $m_s/T=1.0$. In the transition region one finds for the ratio of the fermionic energy densities $\varepsilon_F(m_s/T=1)/\varepsilon_F(m_u/T=0.05)\simeq 0.5$. The good agreement with our ratio of mesonic contributions from strange and nonstrange (pseudo)scalar mesons $[\varepsilon(\text{strange mesons})/\varepsilon(\text{nonstrange mesons})]\sim 0.45$ may be accidental, because the lattice estimate is based on perturbative relations for the energy density. A fully nonperturbative lattice calculation along the lines of Engels *et al.* [31] in a pure SU(3) gauge theory is still outstanding when fermions are included.

VII. SUMMARY OF RESULTS AND CONCLUSIONS

In agreement with the general expectation, results of the high-T expansion are qualitatively correct, but fail quantitatively. The critical temperature in the chiral limit deviates by ~ 85 MeV from T_c in the numerical evaluation, which is applicable also in the transition or crossover region. The crossover region for realistic meson masses is shifted by roughly 80 MeV between the high-T and the numerical results. In our model the high-T expansion practically never reproduces the numerical results in a quantitative way. While the meson condensate $\langle\sigma_0\rangle$ in the realistic mass case has dropped to values $\leqslant 2$ MeV around $T\sim 400$ MeV in the high-T expansion, it is still larger than 30 MeV at this temperature in the numerical calculation. The temperature lies already far outside the applicability range of the model.

The crossover in the light quark condensate looks still rapid for realistic meson masses [$\Delta(\langle\overline{qq}\rangle_T)\sim 50\%$ of $\langle\overline{qq}\rangle_0$ in a temperature interval of 10 MeV in the crossover region]. For the variations in the energy and entropy densities between $181.5\ \mathrm{MeV}\leqslant T\leqslant 192.6$ MeV, we find $\Delta\varepsilon\sim 0.13\pm 0.02\ \mathrm{GeV/fm}^3$ and $T\Delta_s\sim 0.16\pm 0.02\ \mathrm{GeV/fm}^3$. As a loose bound on the latent heat we obtain $0.2\ \mathrm{GeV/fm}^3$, as a more stringent one $0.1\ \mathrm{GeV/fm}^3$, if the change in ε and s would occur over an arbitrarily small temperature interval. The main contributions to the numerical errors, which prevent us from a unique interpretation of the transition or crossover region, come from the uncertainties in the saddle-point value and the minima $\langle\sigma_0\rangle,\langle\sigma_8\rangle$ of $\hat{U}_{\mathrm{eff}}$.

For temperatures above 116 MeV the saddle-point variable gives a positive contribution to the effective masses entering the argument of the logarithm in $\hat{U}_{\mathrm{eff}}$. It increases with temperature. This was one of the reasons why we have chosen the large-N_f expansion. The original hope to completely avoid imaginary parts of $\hat{U}_{\mathrm{eff}}$ in this scheme could not be confirmed by the results. The effective potential is still plagued with imaginary parts for certain regions, where $|\sigma_{0,8}|\leqslant|\langle\sigma_{0,8}\rangle|$ and over the entire temperature range we have studied (up to 250 MeV and above).

The large error bars on ε and s in the transition region may leave some doubts on the smooth nature of the conversion between the chiral symmetric and the chirally broken phase, in particular, because a smooth crossover in the condensates does not automatically imply a smooth change in ε and s. Even if the transition would be of first order, and even if we use a loose bound on the latent heat, it is not larger than $0.2\ \mathrm{GeV/fm}^3$, i.e., 10% of the bag model prediction. To our knowledge it is yet unclear, whether $\Delta L=0.2\ \mathrm{GeV/fm}^3$ latent heat are sufficiently large to induce measurable signatures in heavy-ion experiments, neither is it clear, whether the temperature interval of rapid change is narrow enough. In van Hove's formulation [13] the physical conditions for the occurrence of such signatures are identical for an ideal first-order transition and a rapid crossover phenomenon.

The ratio of critical to realistic current light quark masses has been estimated as $m_{u,d}^{\mathrm{crit}}/m_{u,d}\sim 0.027\pm 0.02$ in mean field and as $m_{u,d}^{\mathrm{crit}}/m_{u,d}\sim 0.26\pm 0.08$ in large N_f, but a ratio of $\approx 30\%$ is probably not large enough to benefit from the vicinity of a second-order phase transition. Because of the fluctuations, which are effectively included in the large-N_f approximation, the ratio in large N_f is at least about half of the lattice result. The *average* pseudoscalar octet masses are 120 MeV and 203 MeV for the realistic ratio of $\varepsilon_0^{\mathrm{crit}}/\varepsilon_8^{\mathrm{crit}}$ in mean field and large N_f, respectively.

The fluctuations we include in our approximation are not likely the only important ones. In particular, it is not clear that they account for fluctuations which induce a renormalization of the quartic and cubic couplings in the Lagrangian.

Recently, it has been raised by Gavin, Gocksch, and Pisarski [15] that the first order of the chiral transition may

be mainly *fluctuation induced.* A fluctuation-induced transition was first discovered by Coleman and Weinberg [34]. It refers to the situation that a system with more than one relevant coupling can have a first-order transition induced by quantum fluctuations.

In our present approach it is difficult to disentangle the driving mechanism for the first-order transition below the critical mass values. A further improvement by including subleading corrections in $1/N_f$ or an ε expansion in $d=4-\varepsilon$ dimensions should clarify, whether the ratio $m_{u,d}^{\mathrm{crit}}/m_{u,d}$ does change to values closer to 1.

A further warning should be mentioned to not take the smooth crossover for granted by the present approach. So far, we have completely neglected the quark and gluonic substructure. In particular, the rearrangement of gluonic degrees of freedom has not been taken into account. The gluonic contribution to the change in entropy and energy densities may well accelerate the crossover process, as we have mentioned in Sec. VI. If the large gap in the entropy density, which has been observed on the lattice, gets further support from larger volume calculations, the disparity with our result indicates the importance of gluonic degrees of freedom. If the discrepancy remains even for frozen gluon dynamics in QCD, it is a manifestation of nonuniversal features in the chiral transition region.

Note also that we have chosen the couplings in the σ model as temperature and energy scale independent over all temperatures up to T_c. In principle, the temperature and scale dependence of the couplings should be derived from QCD rather than being assumed. A less ambitious derivation would start from an effective model underlying the σ model and containing quark and gluonic degrees of freedom. For the critical mass ratio this offers at least a chance for being closer to 1.

ACKNOWLEDGMENT

We would like to thank H.-J. Pirner for useful discussions.

[1] R.D. Pisarski and F. Wilczek, Phys. Rev. D **29**, 338 (1984).
[2] B. Svetitsky and L.G. Yaffe, Phys. Rev. **26**, 963 (1982); Nucl. Phys. **B210** [FS6], 423 (1982).
[3] J. Gasser and H. Leutwyler, Phys. Rep. **87**, 77 (1982).
[4] P. Gerber and H. Leutwyler, Nucl. Phys. **B321**, 387 (1989).
[5] T.A. DeGrand and C.E. DeTar, Nucl. Phys. **B225** [FS9], 590 (1983).
[6] T. Banks and A. Ukawa, Nucl. Phys. **B225** [FS9], 145 (1983).
[7] F.R. Brown, F.P. Butler, H. Chen, N.H. Christ, Z. Dong, W. Schaffer, L. Unger, and A. Vaccarino, Phys. Rev. Lett. **65**, 2491 (1990); see also N.H. Christ, in *Lattice '91,* Proceedings of the International Symposium, Tsukuba, Japan, edited by M. Fukugita *et al.* [Nucl. Phys. B (Proc. Suppl.) **26**, 217 (1992)]; Z. Dong and N.H. Christ, *ibid.,* p. 314.
[8] H. Meyer-Ortmanns, H.J. Pirner, and A. Patkós, Phys. Lett. B **295**, 255 (1992); Int. J. Mod. Phys. C **3**, 993 (1992).
[9] F. Wilczek, Int. J. Mod. Phys. A **7**, 3911 (1992); K. Rajagopal and F. Wilczek, Nucl. Phys. **B379**, 395 (1993).
[10] G. Boyd, J. Fingberg, F. Karsch, L. Kärkkäinen, and B. Petersson, Nucl. Phys. **B376**, 199 (1992).
[11] F. Karsch, Phys. Rev. D **49**, 3791 (1994).
[12] J.-P. Blaizot and J.-Y. Ollitrault, in *Quark-Gluon Plasma,* edited by R.C. Hwa (World Scientific, Singapore, 1990), p. 393.
[13] L. van Hove, Z. Phys. C **27**, 135 (1985).
[14] L.-H. Chan and R.W. Haymaker, Phys. Rev. D **7**, 415 (1973).
[15] S. Gavin, A. Gocksch, and R.D. Pisarski, Phys. Rev. D **49**, R3079 (1994).
[16] D. Metzger, H. Meyer-Ortmanns, and H.-J. Pirner, Phys. Lett. B **321**, 66 (1994); **B328**, 547(E) (1994).
[17] S. Narison, *QCD Spectral Sum Rules,* Lecture Notes in Physics, Vol. 26 (World Scientific, Singapore, 1989), pp. 184, 217.
[18] H. Goldberg, Phys. Lett. B **131**, 133 (1983).
[19] Z. Frei and A. Patkós, Phys. Lett. B **247**, 381 (1990).
[20] S. Coleman, R. Jackiw and H.D. Politzer, Phys. Rev. D **10**, 2491 (1974).
[21] L. Dolan and R. Jackiw, Phys. Rev. D **9**, 3320 (1974).
[22] H.E. Haber and H.A. Weldon, J. Math. Phys. **23**, 1852 (1982).
[23] *Handbook of Mathematical Functions*, edited by M. Abramowitz and I.A. Stegun (National Bureau of Standards, Washington, 1964), p. 375.
[24] *Numerical Recipes*, edited by W.H. Press, B.P. Flannery, S.A. Teukolsky, and W.T. Vetterling (Cambridge University Press, Cambridge, England, 1986), p. 170.
[25] J. Cleymans, A. Kocić, and M.D. Scadron, Phys. Rev. D **39**, 323 (1989).
[26] K. Kajantie, Int. J. Mod. Phys. C **3**, 1137 (1992).
[27] H. Leutwyler, Phys. Lett. B **284**, 106 (1992).
[28] M. Lutz, S. Klimt, and W. Weise, Nucl. Phys. **A542**, 521 (1992).
[29] V. Jain, Nucl. Phys. **B394**, 707 (1993).
[30] T. Hatsuda and T. Kunihiro, Phys. Lett. B **198**, 126 (1987); T. Hatsuda, in *Quark Matter '91,* Proceedings of the Ninth International Conference on Ultrarelativistic Nucleus-Nucleus Collisions, Gatlinburg, Tennessee, edited by T.C. Awes *et al.* [Nucl. Phys. **A544**, 27c (1992)].
[31] J. Engels, J. Fingberg, F. Karsch, D. Miller, and M. Weber, Phys. Lett. B **252**, 625 (1990).
[32] F.R. Brown, N.H. Christ, Y. Deng, M. Gao, and T.J. Woch, Phys. Rev. Lett. **61**, 2058 (1988); Y. Iwasaki, K. Kanaya, T. Yoshié, T. Hoshino, T. Shirakawa, Y. Oyanagi, S. Ichii, and T. Kawai, *ibid.* **67**, 3343 (1991).
[33] J. Kogut and D.K. Sinclair, Phys. Rev. Lett. **60**, 1250 (1988).
[34] S. Coleman and E. Weinberg, Phys. Rev. D **7**, 1888 (1973).